# Enabling the Circular Economy through Chemical Recycling and Upcycling of End-of-Use Plastics

Siddhesh S. Borkar[1,‡], Ryan Helmer[1,‡], Fatima Mahnaz[1], Wafaa Majzoub[2], Waad Mahmoud[2], Ma'moun Al-Rawashdeh[2] & Manish Shetty[1]*

[1]Artie McFerrin Department of Chemical Engineering, Texas A&M University College Station, TX 77843.

[2]Department of Chemical Engineering, Texas A&M University-Qatar, Al-Rayyan, Doha, Qatar.

*Corresponding Author: manish.shetty@tamu.edu

[‡]Authors with equal contributions

## *Summary*

Widespread plastic pollution has led to an environmental crisis, motivating new and effective methods for recycling and upcycling "end-of-use" plastics. In this review, we highlight recent advances in chemical recycling and upcycling pathways, namely, hydroconversion, pyrolysis, and solvent treatment for the deconstruction and valorization of post-consumer plastics. We highlight the advances in the design of supported metal catalysts (Pt, Ru, Zr), for the hydroconversion of plastics, especially polyolefins (PO) and polyesters. We deduce mechanistic insights by comparing and contrasting small alkane and PO hydroconversion reactions. We also review the two types of solvent treatments: chemical solvent treatment (solvolysis) for condensation polymers and solvent extraction for composite polymers. Further, we discuss advances in pyrolysis and cross alkane metathesis to deconstruct POs into liquid hydrocarbons, and finally, the functionalization of POs into vitrimers and adhesives. We highlight the challenges and envision the path forward in optimal catalyst and process design that will enable the development of chemical upcycling technologies for building a circular plastic economy.

**Keywords.** Plastics upcycling, hydroconversion, solvolysis, circular economy, plastics pollution.

# 1. Introduction

Plastics are a vital part of modern life and are ubiquitously found, from single-use polythene bags to life-saving biomedical devices.[1] The first synthetic polymer, Bakelite, was manufactured in the early 20th century. Since then, polymer production has seen exponential growth, reaching ~400 Mmt/yr in 2017 and projected to triple by 2050.[1-3] Ease of production, availability of raw materials from fossil sources, and low manufacturing costs have contributed to the "plastic boom" over the past few decades.[2] The production of monomers accounts for ~7% of global oil and natural gas consumption and has been predicted to increase to 20% in 2050, in line with the increasing demand.[4,5]

According to the United Nations, plastic pollution is on course to double by 2030 and has become an existential challenge for the current generation.[6,7] Only ~25% of single-use plastics, which comprise ~40% of total plastics, are reused.[8] Furthermore, the biodegradation of plastic takes between 20-500 years.[6,7] **Figure 1** shows the current life cycle of plastic waste where 40% of plastics are discarded in landfills, 35% leak into the environment, 16% are incinerated for energy recovery, and only less than 9% are recycled (~3 Mmt out of 36 Mmt of total plastics in 2018 in US).[2,3,8,9]

It is estimated that 4.8–12.7 Mmt/yr of plastic waste enters the oceans and assimilates into the marine environment, forming microplastics and exacting great damage to aquatic life.[10] The inclusion of microplastics in the food chain threatens the health and survival of our biosphere.[11] Removing these oceanic plastics from accumulation zones using ships would need at least 50 years to make any significant impact, and by that time the plastics would have severely degraded to microplastics.[11] To effectively mitigate the environmental release of plastics, it is highly desired to implement strategies for a 'closed-loop-cycle' and shift towards a 'circular economy' for plastics.

Waste plastics represent a lost value of untapped carbon sources that could, if utilized successfully, save up to 3.5 billion barrels of oil every year.[5] The development and deployment of efficient technologies to tap these carbon sources can solve the plastics pollution problem two-fold; first, a circular economy would be created which would save a significant amount of valuable resources, and second, it would contribute to creating new industries and business opportunities.[12,13]

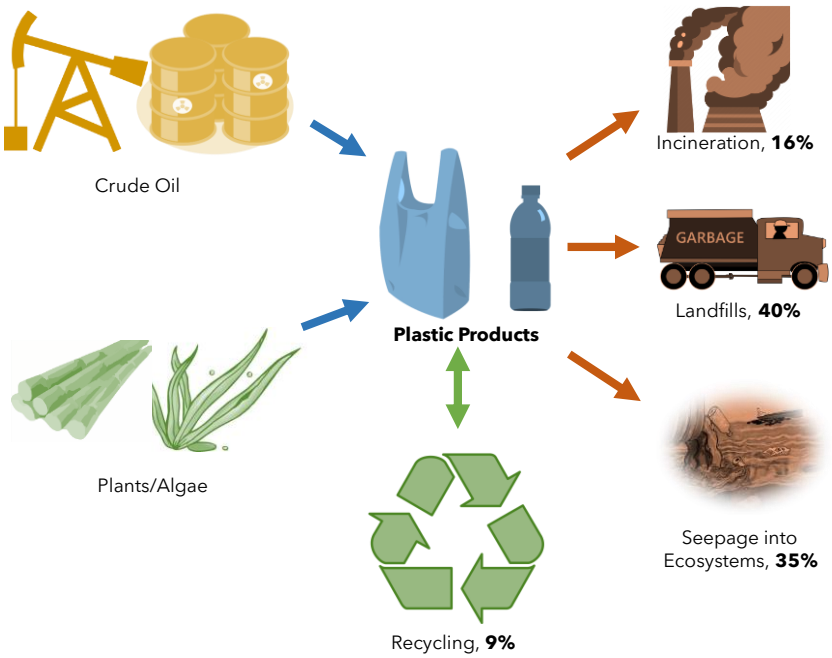


**Figure 1. Linear plastics economy.** Monomers are predominantly produced from fossil sources, along with a small fraction from plant/algae sources. After "end-of-use," plastics are either incinerated, discarded into landfills, seep into ecosystems, or recycled.

One of the first methods of plastic waste recycling is *via* mechanical recycling (secondary recycling), which currently is used to recycle primarily PET and HDPE (29.1% and 29.3% of PET and HDPE, respectively, were recycled in 2018). However, this method often leads to the "downcycling" of plastics into lower-value products.[14] The heat and shear applied during mechanical recycling lead to chain branching, scission, and/or crosslinking of the molecules and degrades the mechanical properties. Contaminants such as pigments, dyes, and volatile components from processing lubricants also alter the chemical, mechanical, thermal, and rheological properties of the polymers and lead to variability in the properties of the recyclate. [15]

Waste plastics are also incinerated (quaternary recycling) with municipal solid waste to harness their calorific value. Incineration destroys most of the plastic waste (solid content is reduced by 90%) and diverts it away from landfills. However, it leads to substantial GHG and toxic emissions. In essence, incineration leads to a loss of valuable carbon and promotes the continual use of fossil resources for plastic production, thereby making this process unfavorable for the development of a true circular plastic economy (**Figure 2**).

The circular economy of plastics through chemical recycling and upcycling (tertiary recycling) of post-consumer plastic has recently attracted interest (**Figure 2)**. This

approach converts "end-of-use" plastics to value-added materials that could be used as monomers to produce new plastics, or as "drop-in" replacements for fossil-derived fuels, lubricants, and waxes. There have been several approaches explored in this regard including, gasification, hydrothermal liquefaction (HTL), pyrolysis, catalytic hydroconversion, and solvent-based depolymerization.

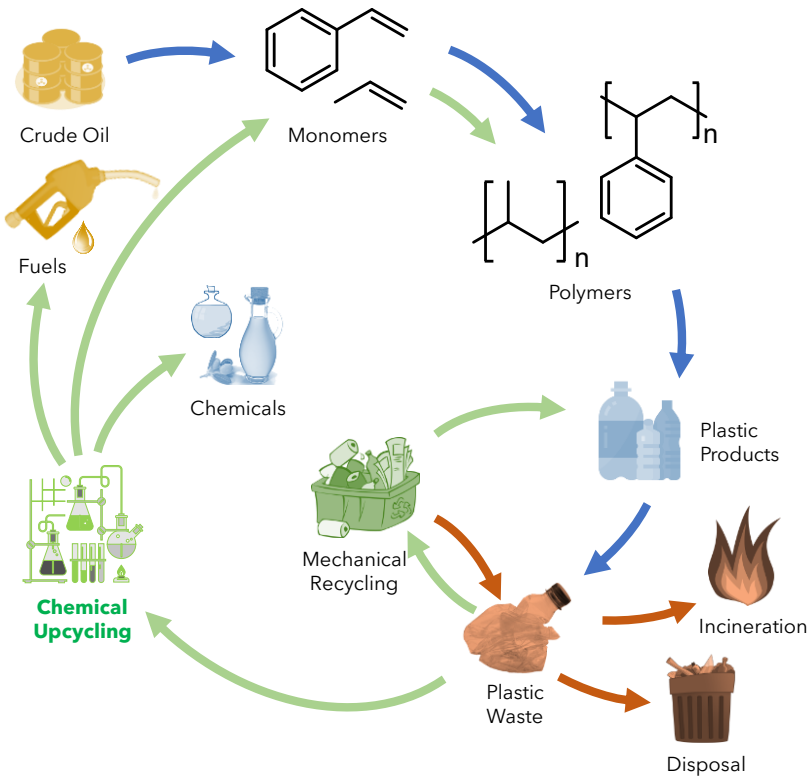


**Figure 2. Circular economy of plastics.** The blue arrows trace the current life cycle of plastics, from fossil sources to plastic products and then discarded (dark orange arrows). The green arrows highlight the mechanical recycling and chemical upcycling approaches to enable the circular economy of plastics.

A potential route for converting plastics into liquid fuels is found in HTL, which applies high temperature (300–550°C) and high pressure (250–300 bar) to convert the polymers into fuel oil.[11] Liquid yields above 90% have been reported using this method, preserving a large plastic fraction in the liquid phase.[11] However, applying severe temperature and pressure leads to high energy consumption and less control over the carbon number distribution in the recovered oil. Partial oxidation or gasification of polymers, using air or steam, is another promising route that has been extensively studied in the literature.[4,16] Its key benefits are the prevention of toxic byproduct formation and the production of *syngas* (carbon monoxide and hydrogen), and hydrocarbons. However, the process involves an additional stage of Fischer-

Tropsch synthesis for the valorization of *syngas* that further requires large energy inputs (temperature between 500-1300°C) and cleanup of the *syngas via* removal of tar.[4,16]

Given the shortcomings of HTL and gasification, plastic upcycling pathways such as pyrolysis, catalytic hydroconversion, and solvent treatment are more promising routes toward a circular economy. They unlock mild operating conditions, potentially making upcycling cost-competitive compared to virgin plastic production, along with emitting lower GHG. In this review, we highlight the progress made in the emerging field of catalytic upcycling of post-consumer plastics, focusing on the routes of catalytic hydroconversion, thermal and catalytic pyrolysis, and solvent-based depolymerization. We specifically focus on catalytic hydroconversion which has emerged as an attractive route to upcycle polyolefins and polyesters. We highlight the advances made in catalyst design and identify emerging trends in catalytic activity, reaction parameters, product selectivity and yield, to inform future catalytic process development. We present insights into depolymerization reaction mechanisms, especially for hydroconversions, and elucidate the nuances associated with hydrocracking and hydrogenolysis. We also highlight the potential of recent advances in thermal and catalytic pyrolysis and solvent-based approaches. Finally, we underline the challenges and opportunities in the field and identify potential solutions and pathways forward.

# 2. Hydroconversion

The hydroconversion reaction, which includes hydrocracking and hydrogenolysis, involves cleavage of the C-C or C-heteroatom (C-O, C-N, *etc.*) bonds in a reacting substrate using $H_2$ gas.[15,17] While a hydrocracking catalyst is bifunctional, with metal and acid sites, a hydrogenolysis catalyst has only metal sites (*vide infra*).[17-19] Recent reports have used hydroconversion to deconstruct plastics into hydrocarbon molecules that can be used as fuels, waxes, and lubricants. These reactions were (predominantly) carried out in a batch reactor with a supported metal catalyst in contact with melt-phase plastics under solvent-free conditions. $H_2$ pressure was varied between 1-50 bar at moderate temperature (150-350°C) and varying contact times (1-48 h). In this section, hydroconversion will first be discussed for polyolefins, followed by polyesters and other plastics. **Table 1** shows the different catalysts, reaction conditions, conversion, and yield data reported for the hydroconversion of plastics.

## 2.1. Polyolefins

Plastics made from polyolefins are the most abundant and their production accounted for more than half of the total global plastics production in 2020 as shown in **Figure 3**.[20] POs are synthesized by the polymerization of olefins such as ethylene,

propylene, styrene, *etc.* and have repeating units connected by aliphatic C-C bonds.[2] Owing to their large production volumes, POs leak into ecosystems at an alarming rate.[3] As such, many of the recent reports on plastic hydroconversion have focused on the most prevalent POs as shown in **Figure 3**, namely, PE (polyethylene) and PP (polypropylene) , with the main objective were to maximize the value of fungible liquid products, and minimizing the gaseous (*e.g.*, methane, ethane) and solid products as shown in **Figure 4**.

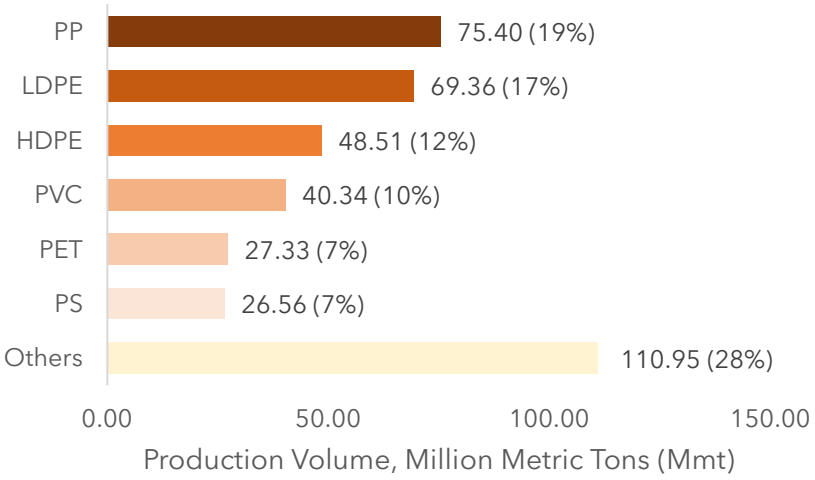


**Figure 3. Global production volumes in million metric tons (Mmt) of polyolefins (POs) in 2020.**[20] The numbers in the brackets represent percentage of total production.

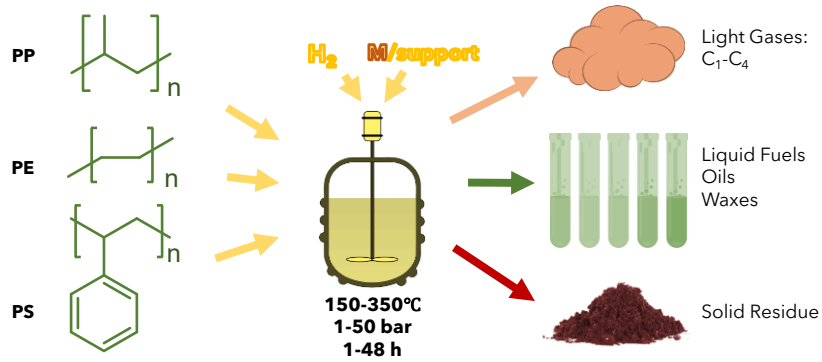


**Figure 4. Typical polyolefin hydroconversion scheme.** The polyolefins undergo hydrogenolysis in the melt phase in a batch reactor at 150-350°C under 1-50 bar $H_2$ pressure and contact time of 1–48 h. Supported metal or bifunctional metal-acid catalysts are typically utilized. The primary targets are the liquid hydrocarbons including aromatics, fuels, lubricants, and waxes, with light gases and solid residues as side products.

For the hydroconversion of waste plastics, both the Pt group (Ru, Rh, Pd, Os, Ir, and Pt) and earth-abundant (Fe, Co, Ni, and Cu) metals have been used.[5,21-24] Among these catalysts, Pt, Zr, and Ru were found to be the most effective. *Ab initio* density functional theory (DFT) calculations have reported these metals to have smaller energy barriers in model alkane C-C bond cleavage.[5,25-27] In the following sections, we highlight the recent advances in hydroconversion of plastics over supported Pt, Zr, and Ru catalysts. We note that all yield and conversion data is reported in mol% herein, unless otherwise mentioned.

### 2.1.1. Platinum (Pt) Catalysts

Platinum (Pt), a widely used hydrogenation and dehydrogenation catalyst, has been keenly studied as a catalyst for PO hydrogenolysis.[28-32] Celik *et al*. reported the transformation of PE into liquid products on Pt supported on $SrTiO_3$ ($Pt/SrTiO_3$) catalyst.[5] At 12 bar $H_2$ and 300°C for 96 h, the hydrogenolysis of PE ($M_n$, number-average molecular weight=8,150, PDI, polydispersity index=2.7) produced a lubricant-like product ($M_n$=590, PDI=1.1) with a 42% yield. Without any catalyst, the $M_n$ reduced from 8,150 to 5,700 and PDI increased from 2.7 to 3.2, suggesting that a catalytic pathway was the dominant hydrogenolysis mechanism for deconstruction. $Pt/SrTiO_3$ also converted a wide variety of other PE samples ($M_n$=~15,000-160,000) to produce similar low $M_n$ alkanes with a narrow dispersion (PDI=1.1-1.3). Surprisingly, the yield of alkanes increased from 42 wt% for the lightest PE, to >99 wt% for the heaviest, suggesting that heavier PEs are more susceptible to hydrogenolysis (*vide infra*). Despite the presence of impurities, the complete conversion of an "end-of-use" plastic bag ($M_n$=33,000) into liquid products ($M_n$=990, PDI=1.3) was achieved.[5] Subsequently, Zhang *et al*. successfully demonstrated the conversion of PE ($M_n$=1,850, PDI=1.90) into liquid linear dialkylbenzenes ($M_n$=414, PDI=1.24) *via* a tandem process of hydrogenolysis/aromatization (without external $H_2$) at 250-330°C on a $Pt/\gamma\text{-}Al_2O_3$ catalyst.[8] Overall, hydrogenolysis produced 75 wt% organic soluble hydrocarbons, 12 wt% insoluble, and 9 wt% gaseous products.

Bates and coworkers used an ultrawide-pore, silica-supported, bimetallic Pt-Re catalyst ($PtRe/SiO_2$) for the hydrogenolysis of perfectly linear HDPE, polystyrene (PS), linear low-density polyethylene (LLDPE), and poly(ethylene-alt-propylene) (PEP).[33] Kinetic analysis and DFT studies pointed towards a degradation mechanism involving C−C chain scission at the tertiary carbon centers associated with short butyl ($-C_4H_9$) branches. Accordingly, at 170°C and 1 h, LLDPE degraded severely ($M_W$, weight-average molecular weight, reduced from 120,000 to under 11,000) while linear HDPE underwent the least chain degradation. Moreover, PS was completely hydrogenated to polycyclohexylethylene (PCHE) due to the absence of tertiary carbon centers.

To overcome the challenges of non-selective C-C bond cleavage on Pt catalysts, a catalytic architecture of mesoporous $SiO_2$ shells surrounding Pt nanoparticles, supported on a solid $SiO_2$ sphere ($mSiO_2/Pt/SiO_2$), was demonstrated to be effective for the hydrogenolysis of "end-of-use" high density polyethylene (HDPE) and isotactic PP (i-PP) into a narrow distribution of liquid hydrocarbons by Tennakoon *et al.* and Wu *et al.*[34,35] Specifically, hydrogenolysis of HDPE at 300°C and 8.9 bar $H_2$ for 15 h gave a narrow $C_{23}$-centered distribution of hydrocarbons. This result was consistent with the processive mechanism, akin to the enzyme-catalyzed processive deconstruction of macromolecules, where PE is suggested to be trapped in mesopores by polymer-surface interactions causing terminal C-C bond cleavage on Pt sites and controlled release of smaller molecular-weight products with a narrow distribution. The mesopore architecture controls the chain scission, thus the resulting size of the hydrocarbon chains was found to be tunable with the mesopore diameter. Furthermore, smaller-sized Pt nanoparticles (1.7 nm) were more reactive at similar reaction conditions than larger particles (2.9 or 5.0 nm).

Vlachos and coworkers have demonstrated hydrocracking on bifunctional Pt catalysts to selectively convert POs to branched liquid fuels (including diesel and gasoline-range hydrocarbons) with a reduction in gas yields. Mechanistically, the polymers undergo tandem catalysis with the activation of polymer over Pt sites first, followed by their cracking *via* β-scission and isomerization to branched hydrocarbons on acid sites, and concluded with the hydrogenation of olefin intermediates over metal sites (*vide infra*).[36] Accordingly, branched alkanes were produced with negligible gas yields from LDPE ($M_w$~76,000) using bifunctional Pt deposited on tungstated zirconia ($Pt/WO_3/ZrO_2$) at 250°C and 30 bar $H_2$ for 1-24 h. The metal-to-acid site molar ratio (MAB) (varied with the Pt and $WO_3$ content) had a substantial effect on the product selectivity. By increasing MAB ratio from 0.06 to 0.86, the ratio of $C_{21+}/C_{4-6}$ increased from ~0.05 to ~0.7. It was hypothesized that at a high MAB ratio, olefins and paraffins establish pseudo-equilibrium with the metal sites, and the slow acid-catalyzed reactions lead to deep isomerization before β-scission. At a low MAB ratio, isomerization and cracking occur through a parallel β-scission pathway that leads to a higher extent of C-C cleavage.[37]

A high yield (~60-85%) towards branched, liquid fuels was demonstrated by Liu *et al.* at 250°C and 30 bar $H_2$ over a $Pt/WO_3/ZrO_2$ and HY zeolite mixture for a number of plastics, including LDPE ($M_w$= 250,000), i-PP ($M_w$= 250,000), HDPE, PS ($M_w$= 35,000), mixed layered plastics, bottles, and transparent bags (**Figure 5B**).[36] In another study, a bifunctional mechanism was indicated by the conversion of LDPE into liquid alkanes ($C_5$-$C_{13}$) at 63.6 wt% yield along with an overall light alkane ($C_1$-$C_{13}$) yield of 94 wt% at 250°C and 30 bar $H_2$ for 1 h on $Pt/WO_3$/β-zeolite. The catalyst produced a narrow range of gasoline grade alkanes from LLDPE, HDPE, and PP with liquid product yields as high as 74.5 wt% for HDPE.[38]

Utami *et al.* used Pt-promoted sulfated zirconia (Pt/SZr) to convert pyrolized LDPE into liquid hydrocarbons with a 74.60 wt% yield (0.15% solid and 25.25% gas) in a flow-reactor at 250°C and 1 bar $H_2$ for 1 h. The liquid product had 67.5 wt% of hydrocarbons in the gasoline range ($C_5$-$C_{12}$) and 7.1 wt% in the diesel range ($C_{13}$-$C_{20}$).[39] Furthermore, a higher acidity of the catalyst, controlled with Pt loading, was found to be concomitant with higher yields of gasoline-range hydrocarbons ($C_5$-$C_{12}$).

Overall, supported Pt has been shown to be an active hydroconversion catalyst for the conversion of PO to fungible hydrocarbons at high yields under mild conditions.

### 2.1.2. Zirconium (Zr) Catalysts

A breakthrough in polymer synthesis was made by Ziegler and Natta in the 1950s when they discovered transition metal Ziegler-Natta catalysts for the polymerization of terminal olefins (α-olefins), ethylene, and propylene.[40] The Ziegler-Natta catalyst typically consists of transition metals with organometallic compounds, such as $Al(C_2H_5)_3$, as cocatalysts, immobilized on a support.[41] As the scale-up of this technology enabled the plastic boom, researchers began exploring catalysts for their depolymerization. Using the microscopic reversibility of Ziegler-Natta polymerization, transition metals akin to Ziegler-Natta catalysts were used to break-down POs into lower aliphatic hydrocarbons.[42]

Basset and coworkers demonstrated the efficacy of a $SiO_2$-supported zirconium hydride, $(\equiv SiO)_3ZrH$, grafted by organometallic chemical reactions, to cleave C-C bonds under atmospheric pressure and mild temperatures (25-150°C).[43] Zirconium hydride catalyst with $SiO_2$-$Al_2O_3$ support was reported to convert PE and PP to lower alkanes ($C_1$-$C_{17}$) at low temperature (150°C) and 1 bar $H_2$. After 5 h, all the PEs ($C_{20}$-$C_{50}$, $M_W$=280–700) were converted to $C_1$-$C_{17}$ products. Longer reaction times (62 h) converted PE to lighter alkanes, eventually forming methane.[21] Heavier LDPE ($M_W$=125,000) showed 100% conversion to saturated oligomers at 150°C after 5-10 h. In addition, 40% of commercial i-PP ($M_W$=250,000) was converted into lower alkanes ($C_1$-$C_7$) at 190°C after 15 h.

An electrophilic (cationic) single-site organozirconium Zr-alkyl catalyst deposited on Brønsted-acidic sulfated alumina support, Zr[neopentyl]$_2$AlS, was shown to rapidly cleave C-C bonds in saturated hydrocarbons and a variety of plastics, namely, PE, i-PP, PE-co-1-octene (PECO), and a waste PE sandwich bag. Specifically, the supported Zr-H species produced $C_1$-$C_{12}$ alkanes from *n*-hexadecane, at 150°C and ~2.5 bar $H_2$ in 0.3 h. Under similar conditions (150-190°C and 2 bar $H_2$), an overall PE conversion of 95 wt% was observed after 2 h. PECO and i-PP both showed >96 wt% overall conversion after 1 h whereas the PE sandwich bag took about 24 h to reach a comparable 96 wt% conversion.[27] In summary, Zr-based catalysts show promise to hydrogenolytically cleave C-C bonds in POs.

### 2.1.3. Ruthenium (Ru) Catalysts

Ruthenium-metal catalysts have been reported to be the most active for hydrogenolysis of a variety of hydrocarbons.[44,45] Notably, Almithn and Hibbitts reported through DFT calculations that the free-energy barrier for C-C bond cleavage of quasi-equilibrated dehydrogenated species from ethane (*CH-CH*) was the lowest for Ru among Group 8-11 transition metals for ethane hydrogenolysis.[25] Furthermore, Ru has been reported to be effective on both neutral (*e.g.*, Ru/C) and metal-oxide supports (*e.g.*, $Ru/TiO_2$, $Ru/CeO_2$) for PO hydrogenolysis.[24,46-48]

Roman and coworkers focused on the catalytic hydrogenolysis of PE and PP to liquid alkanes.[24,48] First, a series of metal and metal-oxide catalysts were investigated for the hydrogenolysis of *n*-octadecane (as a model PE), namely, Pt/γ-$Al_2O_3$, Ni/C, γ-$Al_2O_3$, NiO, $Co_3O_4$, $RuO_2$, Rh/C, $Ru/Al_2O_3$, and Ru/C under mild conditions (200-250°C, 20-50 bar $H_2$) for 14 h. 5 wt% Ru/C was identified as the most suitable catalyst with 92 wt% conversion to produce *n*-alkanes ($C_6$-$C_{17}$) and gaseous light alkanes ($C_1$-$C_5$) at high yields. For low molecular weight PE ($M_w$=4,000), 200°C and 22 bar $H_2$ were optimum for producing liquid alkanes ($C_8$-$C_{45}$). A gradual shift in product distribution towards light gases (similar yields of methane, ethane, and propane at 200°C; 3:1 ratio of methane to ethane at 225°C; and pure methane at 250°C) was observed as the reaction time was extended. The residue of solid products was also suppressed by increasing $H_2$ pressure from 15 bar to 20 bar, with any further $H_2$ pressure increase not leading to any variation in product distribution (**Figure 5A**).

To further demonstrate the efficacy of the catalyst, an LDPE (melt index 25 g/10 min), and a post-consumer LDPE bottle were converted by the Ru/C catalyst to liquid alkanes ($C_8$-$C_{45}$). Furthermore, two PP feedstocks ($M_w$=12,000 and 340,000) over the same catalyst under similar conditions produced liquid *iso*-alkanes ($C_5$-$C_{42}$). The former produced 68 wt% of liquid *iso*-alkanes at 225°C and 20 bar $H_2$ over 16 h while the latter required harsher conditions (225°C and 50 bar $H_2$ over 24 h) for achieving a similar product distribution. Notably, the recycled catalyst showed minimal change in its activity for both PE and PP. A mixed substrate stream of PP and HDPE at 225°C under 40 bar $H_2$ for 24 h produced a distribution of linear alkanes ($C_5$-$C_{13}$) and branched alkanes ($C_7$-$C_{32}$), enhancing their suitability in making diesel fuel blends.[49] Recently, Lin and coworkers demonstrated the effectiveness of the 5 wt% Ru/C in the presence of *n*-hexane as a solvent to produce maximum yields of 60.8 wt% and 31.6 wt% towards jet-fuel ($C_8$-$C_{16}$) and lubricant-range liquid hydrocarbons ($C_{23}$-$C_{38}$), respectively from HDPE plastic at 220°C and 20-30 bar $H_2$. The maximum yield of liquid hydrocarbon products reached about 90 wt% within 1 h at 220°C and 60 bar of $H_2$.[44]

Nakaji *et al.* employed LDPE ($M_w$=4,000) for screening metals on reducible $CeO_2$ support (M/$CeO_2$, M=Ru, Ir, Rh, Pt, Pd, Cu, Co, Ni) at 240°C and 60 bar $H_2$ for 5 h.[47] Only $Ru/CeO_2$ showed an LDPE conversion of 76% at 5 h. The conversion increased to 99%

at 8 h, with a total liquid yield of 90% (84% fuel and 7% wax) (**Figure 5C**). Ru on other metal-oxide supports ($TiO_2$, MgO, $ZrO_2$, $SiO_2$) and neutral carbon supports gave moderate conversions (66-83%) and liquid yields (39-73%). Importantly, $Ru/CeO_2$ was effective for converting LDPE ($M_w$=4,000-50,000), HDPE ($M_w$=64,000), PP ($M_w$=12,000), a plastic bag ($M_w$=177,000), and waste PEs at >99% conversions and yields for liquid fuels and waxes in the range of 83-91%.

A key disadvantage of Ru/C is the formation of light gases from POs, reducing liquid hydrocarbon yields. However, $Ru/TiO_2$ was shown to be a viable catalyst in the conversion of PP to lubricants with high liquid yields under modest conditions.[46] Different samples of PP produced over 59 wt% liquid yields at 250°C and 30 bar $H_2$ for 12-24 h over $Ru/TiO_2$, and the liquid products showed comparable physical properties to commercial lubricants. In contrast, Ru/C and $Ru/CeO_2$ formed light gases ($C_1$-$C_6$) under identical reaction conditions.

Ru supported on tungstated-zirconia (Ru-WZr) also significantly suppressed methane formation and produced diesel and wax/lubricant base oil ($C_5$-$C_{35}$) from LDPE ($M_w$=76,000) under mild conditions (250°C, 50 bar $H_2$) and low reaction times (< 2 h) (**Figure 5D**). Crucially, this was unachievable on other acidic supports, such as, Zr, WSi, HY zeolite, and mesoporous [Al]MCM-41.[50] The controlled hydrogenolysis was attributed to the capacity of $(WO_x)_n$ clusters to store H as surface hydroxyls by spillover, and this was hypothesized to be pivotal in the desorption of long alkyl intermediates that would otherwise undergo further C−C scission to produce methane. High liquid yields were also achieved on post-consumer LDPE bottles (73% liquid, 18% gas), cling wrap (67% liquid, 21% gaseous), and lab pipettes (40% liquid, 12% gas).[50] Interestingly, unlike bifunctional Pt catalysts, Ru on acidic supports did not show any evidence of a bifunctional mechanism (*vide infra*).

PS was depolymerized into a variety of arenes over $Ru/Nb_2O_5$ at 300°C and 5 bar $H_2$ for 16 h.[51] The C-C bond of the $sp^2$-$sp^3$ bond connecting the aliphatic backbone to the phenyl groups was selectively cleaved to yield 76% of monocyclic arenes, despite the potential of hydrogenating the phenyl groups.[52] As such, PS was largely converted into benzene (~50% yield), along with ethylbenzene (~8% yield). Overall, supported Ru catalysts exhibited activity for hydrogenolysis of POs, even in the presence of acidic supports. **Figure 5** highlights some of the key findings from a few of the above reports.

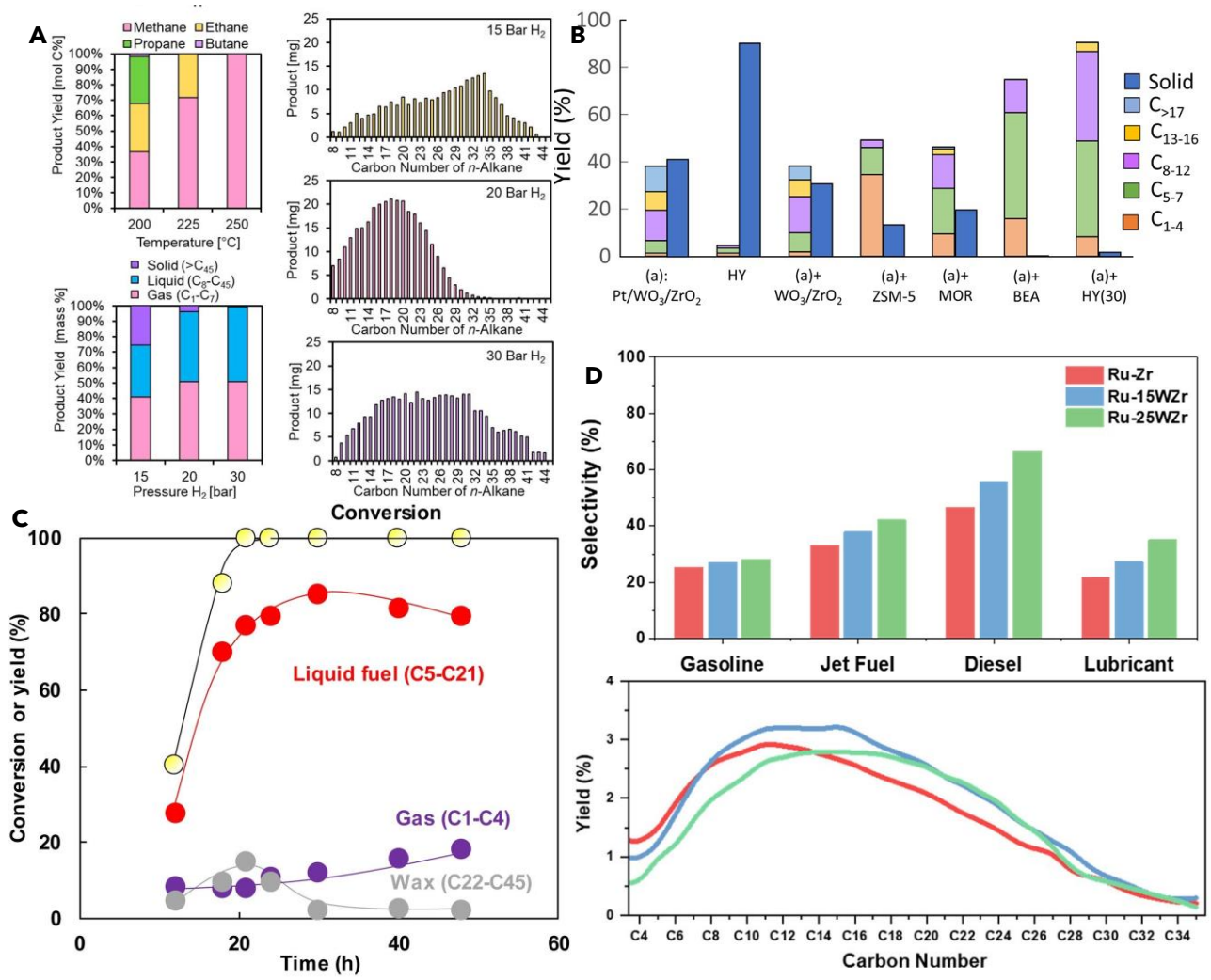


**Figure 5. General trends in polyolefin hydroconversion. A.** Solid, liquid, and gas product yields (Left) and corresponding liquid product distributions (Right) from hydrogenolysis of PE ($M_w$=4,000). Reaction conditions (Top-left): 100 mg PE, 25 mg 5 wt% Ru/C catalyst, 30 bar $H_2$, 16 h; (Other plots): 700 mg PE, 25 mg 5 wt% Ru/C catalyst, 200°C, 16 h. Reprinted with permission from Rorrer *et al.*[24] Copyright 2020, The Authors. Published by American Chemical Society. **B.** Effect of different supports on the product distribution in the hydrocracking of LDPE. Reaction conditions: 2 g LDPE, 0.2 g catalyst, 250°C, 30 bar $H_2$, 2 h. Reprinted with permission from Liu *et al.*[36] Copyright 2021, The Authors. **C.** Product yields with reaction time in h from LDPE hydrogenolysis ($M_w$=4,000) over $Ru/CeO_2$ catalyst. Reaction conditions: 3.4 g PE, 500 mg 5 wt% $Ru/CeO_2$ catalyst, 200°C, 20 bar $H_2$, 12-48 h. Reprinted with permission from Nakaji *et al.*[47] Copyright 2020, Elsevier. **D.** Effect on gasoline, jet fuel, diesel, and lubricant selectivity with varied $WO_x$ loading in Ru-WZr catalysts on LDPE hydrogenolysis. (Top) Selectivities by fuel range: gasoline, $C_5$–$C_{12}$; jet fuel, $C_8$–$C_{16}$; diesel, $C_9$–$C_{22}$; and waxes/lubricant base-oils, $C_{20}$–$C_{35}$. (Bottom) Detailed carbon distributions of the non-solid products. Reaction conditions: 2 g LDPE, 50 mg catalyst,

250°C, 50 bar $H_2$, 2 h. Reprinted with permission from Wang *et al.*[50] Copyright 2021, The Authors. Published by American Chemical Society.

## 2.2. Polyesters

Polyesters are synthesized by the condensation of alcohols and carboxylic acids. Some of the common examples of polyesters are polyethylene terephthalate (PET), polylactic acid (PLA), polyhydroxybutyrate, polyethylene adipate, and polybutylene terephthalate. Among them, PET is the most abundantly produced polyester, with a production of ~27.3 Mmt in 2020.[20] PET is made from the polycondensation of terephthalic acid (TPA) and ethylene glycol (EG). Consequently, a natural upcycling pathway is its depolymerization into monomers, TPA and EG.[53]

The Milstein catalyst, an Ru coordination compound (**Figure *6***) is a versatile catalyst to synthesize esters and amides from the dehydrogenative coupling of alcohol and alcohol-amine pairs, respectively.[54] In contact with $H_2$ gas, the catalyst is activated for the reverse reaction, *i.e.*, hydrogenation of esters to their corresponding alcohols.[55] Accordingly, milled PET from a used water bottle was hydrogenated into *p*-xylene glycol and EG at a conversion of above 99% in an anisole/THF solvent at 160°C and 55 bar $H_2$ for 24 h.[56]

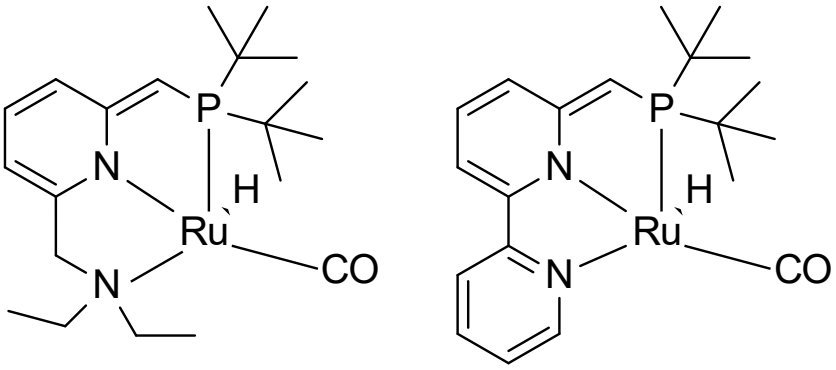


Milstein Catalyst #2 Milstein Catalyst #4

**Figure 6. Structure of the Milstein Catalysts that are active for polyester hydroconversion.** Adapted with permission from Krall *et al.*[56] Copyright 2014, The Royal Society of Chemistry.

PET was also deconstructed to TPA and ethylene in a solvent-free hydrogenolysis pathway using carbon-supported molybdenum-dioxo complex ($MoO_2$/C). The depolymerization was achieved at 1 bar $H_2$ pressure and 260°C, with 87% yield to TPA.[23] Yan and coworkers performed catalytic hydroconversion of PET to arenes using a Co/$TiO_2$ catalyst. First, a pure TPA monomer was converted mainly to xylene and toluene with yields of 75% and 9%, respectively, at 340°C and 30 bar $H_2$ pressure for 4

h (**Figure 7B**). Under similar conditions, PET formed xylene and toluene at 79% combined yield after 24 hr. However, a loss of catalytic activity was reported in the recyclability study due to Co leaching and the degradation of $TiO_2$ crystallinity.[22] Along with the hydrogenolysis of PS into benzene, Yan and coworkers demonstrated the use of $Ru/Nb_2O_5$ in converting several aromatic plastics (PET, PS, poly(p-phenylene oxide) (PPO), and PC) into arene monomers. For PET alone, the catalyst gave a yield of 95.2% $C_6$-$C_8$ products. When applied to an equal mixture of PET, PS, PPO, and PC, the catalyst yielded 78.9% $C_6$-$C_{10}$ arene products. Direct conversion of a PET waste bottle produced 90.9% $C_6$-$C_8$ yield (78.4% arenes) at 200°C and 3 bar $H_2$ pressure for 8 h (**Figure 7A**). In contrast, Pd and Pt on $Nb_2O_5$ support produced cycloalkanes, due to secondary hydrogenation of the arenes. [51]

Poly(butylene succinate) (PBS) is a bio-degradable polyester that degrades to $CO_2$ and water between 6-10 months at 25-50°C. Pyrolysis of PBS was reported to produce a mixture of succinic acid, succinic anhydride, and tetrahydrofuran (THF), albeit at high temperatures above 400°C.[57] In search of milder reaction conditions, catalytic hydrogenolysis over Pd/C was used to selectively produce THF at 240°C and 60 bar $H_2$, at 53-60 wt% yield after 12-36 h.[58]

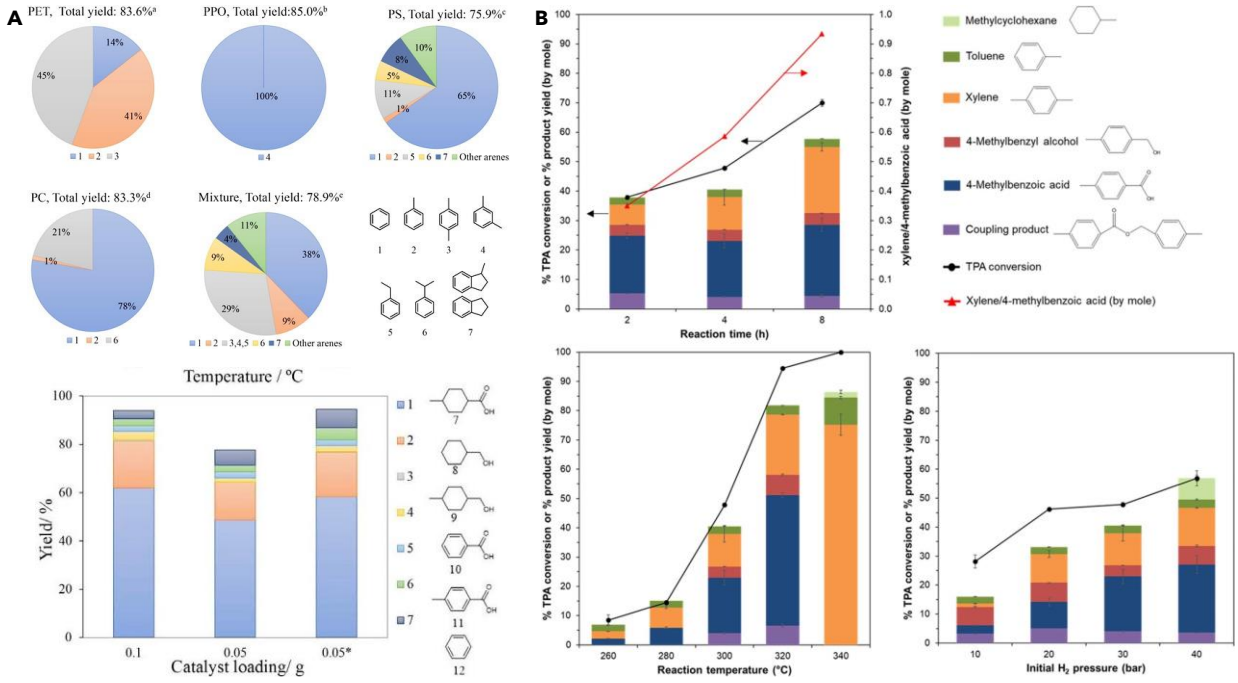


**Figure 7. General trends from polyester hydroconversion. A.** (Top) Product distributions from hydrogenolysis of aromatic plastics over $Ru/Nb_2O_5$. Reaction conditions: 30 mg feed, 30 mg $Ru/Nb_2O_5$ catalyst, 4 g octane, 5 bar $H_2$. PET: 280°C, 8 h; PPO: 280°C, 16 h; PS: 300°C, 16 h; PC: 320°C, 16 h; Mixed Feed: 15 mg PET, 15 mg PC, 15 mg PS, 15 mg PPO, 60 mg $Ru/Nb_2O_5$ catalyst, 4 g octane, 320°C, 5 bar $H_2$, 16 h. (Bottom) Product yields with varied catalyst loading. Reaction conditions: 0.1 g PET, 10

g $H_2O$, 200°C, 3 bar $H_2$, 8 h (*16 h). Reprinted with permission from Jing *et al.*[51] Copyright 2020, Wiley-VCH GmbH. **B.** Effect of reaction parameters on TPA conversion and product yields obtained from hydrodeoxygenation of TPA over Co/$TiO_2$ catalyst: (Top) reaction time, (Bottom-left) reaction temperature, and (Bottom-right) initial $H_2$ pressure. Reaction condition: 30 bar initial $H_2$, 300°C, 4 h. Reprinted with permission from Hongkaillers *et al.*[22] Copyright 2021, Wiley-VCH GmbH.

## 2.3. Other Plastics

Hydrogenolysis has also been reported to be effective on squalane, a $C_{30}$ algae-derived branched hydrocarbon. Tomishige and coworkers showed that Ru supported on C, $SiO_2$ and $CeO_2$ were promising catalysts for the hydrogenolysis of squalane to smaller hydrocarbons without isomerization and aromatization. Pt/C, Pd/C, Rh/C, and Ir/$SiO_2$ catalysts showed negligible reactivity at 240°C and 35 bar $H_2$ pressure for *n*-hexadecane as a model substrate. In contrast, under identical conditions, Ru/C, Ru/$SiO_2$ and Ru/$CeO_2$ showed high reactivity (TOF, 79 $h^{-1}$, 180 $h^{-1}$ and 39 $h^{-1}$, respectively). Ru/$CeO_2$ was further used to hydrogenolyze squalane to a yield of 40% of either $C_{9-10}$ or $C_{14-16}$ products, depending on reaction time, demonstrating its capability of product selectivity.[59] The absence of light gases at low reaction times proved that the internal non-terminal $H_2C$-$CH_2$ bonds were preferentially cleaved over terminal C-C bonds. In another study, vanadium (V) was also added to Ru to reduce the terminal C-C bond cleavage at longer reaction times. It was proposed that V species cover Ru particles and reduce the number of Ru ensembles that are active for terminal C-C cleavage. This effect was most remarkable on $SiO_2$ support. Ru-$VO_x$/$SiO_2$ (V/Ru = 0.25 mol) showed lower methane selectivity than Ru/$SiO_2$ and the highest $C_{14-16}$ selectivity among Ru/$SiO_2$, $VO_x$/$SiO_2$, $VO_x$/$CeO_2$, $VO_x$/MgO, $VO_x$/$TiO_2$, and $VO_x$/$ZrO_2$.

Li and coworkers demonstrated the applicability of a mixture of Rh/C and H-USY zeolite for the conversion of PC. A 94.9% yield of propane-2,2-diyldicyclohexane was reported over PC pellets at 200°C and 35 bar $H_2$ after 12 h, which shows the potential for producing jet fuel blends from PC. Under identical conditions, a waste DVD disk (PC) yield 86.9% propane-2,2-diyldicyclohexane.

**Table 1** below (see Table S1 for detailed information) provides a comparative overview of hydroconversion catalysts and the influence of key reaction parameters such as, catalyst loading, reaction temperature/pressure, and substrate type on the yield and selectivity of upcycled liquid products.

**Table 1**. Summary of recent works on the hydroconversion of polyolefins. The table highlights the substrate/polyolefins, catalyst, and reaction parameters, and nature and quantitation of product yields.

| Substrate | Catalyst | Catalyst Metal Loading (wt%) | Catalyst /Feed Ratio (wt) | Temp (°C) | Pressure (bar) | Time (h) | Product(s) of Interest | Product $C_N$ | Product Yield (mol%) | Ref. |
|---|---|---|---|---|---|---|---|---|---|---|
| PE ($M_w$=22000) | $Pt/SrTiO_3$ | 11.10% | 0.200 | 300 | 12 | 96 | Waxes and lubricants | $C_{42}$[a] | 42%[b] | 5 |
| PE ($M_w$=17000) | | | | 300 | 12 | 96 | | $C_{47}$[a] | 68%[b] | |
| PE ($M_w$=70000) | | | | 300 | 12 | 96 | | $C_{57}$[a] | 91%[b] | |
| PE ($M_w$=420000) | | | | 300 | 12 | 96 | | $C_{59}$[a] | >99%[b] | |
| Plastic bag | | | | 300 | 12 | 96 | | $C_{70}$[a] | 97%[b] | |
| PE ($M_w$=3500) | $Pt/\gamma\text{-}Al_2O_3$ | 1.50% | 1.667 | 280 | N/A | 24 | Alkylaromatic Liquids; Waxes | $C_{30}$[a] | 75%[b] | 8 |
| PE ($M_w$=3500) | | | | 280 | N/A | 24 | | $C_{34}$; $C_{39}$[a] | 70% (46%; 24%)[b] | |
| LDPE bag | | | | 280 | N/A | 24 | | $C_{27}$; $C_{26}$[a] | 69% (39%; 30%)[b] | |
| HDPE bottle cap | | | | 280 | N/A | 24 | | $C_{20}$; $C_{35}$[a] | 55% (20%; 35%)[b] | |
| LLDPE | $PtRe/SiO_2$ | [c] | 1.000 | 170 | 35 ($D_2$) | 17 | Lower *n*-alkanes ($M_w$~6000) | $C_{179}$[a] | [c] | 33 |
| HDPE | | | | 170 | 35 ($D_2$) | 17 | Lower *n*-alkanes ($M_w$~98000) | $C_{1666}$[a] | [c] | |
| PEP | | | | 170 | 35 ($D_2$) | 17 | Lower PEP ($M_w$~74000) | $C_{4400}$[a] | [c] | |
| PS | | | | 170 | 35 ($D_2$) | 17 | PCHE ($M_w$~88000) | $C_{6100}$[a] | [c] | |
| PE ($M_w$=90000) | $mSiO_2/Pt/SiO_2$ | 0.085% (1.7 nm) | 0.0085 | 300 | 8.9 | 15 | Wax | $C_8$-$C_{36}$ | 74%[b] | 34,35 |
| i-PP | | | | 300 | 8.9 | 12 | | | 73%[b] | |

| | | | | | | | | | | |
|---|---|---|---|---|---|---|---|---|---|---|
| LDPE | $Pt/WO_3/ZrO_2$ | 0.5% Pt; 15% $WO_3$ | 0.100 | 250 | 30 | 12 | Fuels and Lubricants | $C_4$-$C_{30}$ ($C_7$-$C_{12}$) | >99% (65.2%) | [37] |
| LDPE | $Pt/WO_3/ZrO_2$ + HY(30) (Phys. mixture) | 0.5% Pt; 15% $WO_3$ | 0.100 | 250 | 30 | 2 | Liquid fuels (Gasoline, diesel) | $C_5$-$C_{22}$ ($C_5$-$C_{12}$, $C_8$-$C_{22}$) | 82% (78%, 42%) | [36] |
| i-PP | | | | 250 | 30 | 2 | | | 82% (74%, 53%) | |
| i-PP/LDPE/PS | | | | 250 | 30 | 4 | | | 68% (63%, 41%) | |
| LDPE | $Pt/WO_3$/Beta | 2% Pt; 0.5% W | 0.025 | 250 | 30 | 1 | Light Gasoline | $C_5$-$C_{13}$ | 63.60%[b] | [38] |
| LLDPE | | | | 250 | 30 | 1 | | | 65.00%[b] | |
| HDPE | | | | 250 | 30 | 1 | | | 74.50%[b] | |
| PP | | | | 250 | 30 | 1 | | | 52.30%[b] | |
| LDPE | $Pt/SZrO_2$ | 1.50% | 0.010 | 250 | 1 bar; 20mL/min | 1 | Liquid fuels | $C_5$-$C_{20}$ ($C_5$-$C_{12}$, $C_{13}$-$C_{20}$) | 74.60% (67.5%, 7.1%)[b] | [39] |
| PE (HMW) | $ZrH(SiO)_3$ | 3% | 0.000 | 150 | 1 | 5 | Oligomers | $C_{10}$-$C_{17}$ | 100% | [21] |
| i-PP | | | | 190 | 1 | 15 | Light gases | $C_1$-$C_7$ | 40% | |
| PE | $ZrNp_2/SAl_2O_3$ | 1.4% Zr | 0.150 | 150 | 2 | 0.83 | *n*-alkanes | $C_{10}$-$C_{26}$ | 43%[b] | [27] |
| i-PP | | | | 190 | 2 | 1 | branched-alkanes | $C_{10}$-$C_{30}$ | 68% | |
| PECO | | | | 190 | 2 | 1 | *n*-alkanes | $C_{12}$-$C_{22}$ | 15%[b] | |
| PE (model) | 5% Ru/C | 5% | 0.040 | 200 | 22 | 14 | *n*-alkanes | $C_8$-$C_{45}$ | 45%[b] | [24] |
| PE (LLDPE) | | | 0.050 | 225 | 22 | 16 | *n*-alkanes | $C_8$-$C_{20}$ | 53%[b] | |
| LDPE | | | 0.036 | 225 | 22 | 16 | *n*-alkanes, branched alkanes | $C_8$-$C_{45}$ | 48%[b] | |
| LDPE Bottle | | | 0.125 | 225 | 22 | 2 | *n*-alkanes, branched alkanes | $C_8$-$C_{45}$ | 48%[b] | |
| i-PP (LMW) | 5% Ru/C | 5% | 0.143 | 225 | 20 | 16 | iso-alkanes | $C_8$-$C_{42}$ | 68%[b] | [48] |
| i-PP (HMW) | | | 0.071 | 250 | 40 | 8 | | $C_5$-$C_{32}$ | 35%[b] | |
| i-PP (HMW) | | | 0.071 | 225 | 50 | 24 | | $C_5$-$C_{32}$ | 39%[b] | |

| | | | | | | | | | | |
|---|---|---|---|---|---|---|---|---|---|---|
| HDPE/i-PP | | | 0.036 | 225 | 40 | 24 | *n*-alkanes, branched-alkanes | $C_5$-$C_{32}$ | 25%[b] | |
| HDPE | 5% Ru/C | 5% | 0.500 | 220 | 30 | 1 | Jet fuels; diesel fuels | $C_8$-$C_{38}$ ($C_8$-$C_{16}$, $C_{17}$-$C_{22}$) | 75% (61%, 14%)[b] | 44 |
| HDPE | | | 0.500 | 220 | 60 | 1 | Jet fuels; lubricant hydrocarbons | $C_8$-$C_{38}$ ($C_8$-$C_{16}$, $C_{23}$-$C_{38}$) | 87% (38%, 18%)[b] | |
| LDPE | $Ru/CeO_2$ | 5% | 0.029 | 240 | 60 | 8 | Liquid Fuels, Wax | $C_5$-$C_{45}$ ($C_5$-$C_{21}$, $C_{22}$-$C_{45}$) | 90% (84%, 7%) | 47 |
| LDPE | | | | 240 | 60 | 18 | | | 88% (82%, 5%) | |
| LDPE | | | | 240 | 60 | 24 | | | 87% (80%, 7%) | |
| HDPE | | | | 240 | 60 | 10 | | | 87% (83%, 4%) | |
| PP | | | 0.059 | 240 | 60 | 72 | | | 83% (72%, 10%) | |
| Plastic Bag/LDPE | | | 0.147 | 200 | 20 | 30 | | | 91% (87%, 4%) | |
| Waste PE/ LDPE | | | | 200 | 20 | 48 | | | 88% (87%, 2%) | |
| i-PP (HMW) | $Ru/TiO_2$ | 5.90% | 0.050 | 250 | 30 | 16 | Oil | $C_{49}$ avg, $C_7$-$C_{200}$[a] | 66%[b] | 46 |
| i-PP (HMW) | | | 0.025 | 250 | 30 | 24 | | $C_{87}$ avg, $C_7$-$C_{760}$[a] | 73%[b] | |
| i-PP (LMW) | | | | 250 | 30 | 12 | | $C_{122}$[a] | 80%[b] | |
| a-PP | | | | 250 | 30 | 16 | | $C_{159}$[a] | 71%[b] | |
| PP bag | | | | 250 | 30 | 16 | | $C_{105}$[a] | 68%[b] | |
| PP bottle | | | | 250 | 30 | 20 | | $C_{164}$[a] | 59%[b] | |
| LDPE | $Ru\text{-}15WZrO_2$ | 5% | 0.025 | 250 | 50 | 2 | Fuels and Lubricants, | $C_5$-$C_{35}$ | 60% | 50 |
| LDPE Bottle | | | | 250 | 50 | 2 | | | 73% | |

| | | | | | | | | | | |
|---|---|---|---|---|---|---|---|---|---|---|
| LDPE Cling Wrap | | | | 250 | 50 | 1.5 | normal & branched | | 67% | |
| LDPE Pipette | | | | 250 | 50 | 1.25 | | | 40% | |
| PET | $Ru/Nb_2O_5$ | 2% | 1.000 | 200 | 3 | 12 | Aromatics, Cycloalkanes | $C_6$-$C_8$ | 95% | 51 |
| PET | | | | 280 | 5 | 8 | Aromatics (BTX, EB, Cumene, etc.) | $C_6$-$C_{10}$ | 84% | |
| PPO | | | | 280 | 5 | 16 | | | 85% | |
| PS | | | | 300 | 5 | 16 | | | 76% | |
| PC | | | | 320 | 5 | 16 | | | 83% | |
| PET/PPO/PS/PC | | | | 320 | 5 | 16 | | | 79% | |
| Polyester (model) | Milstein catalyst #2 | - | 0.028 | 120 | 13.8 | 24 | 1,10 decane diol | $C_{10}$ | 80% | 56 |
| PET (bottle) | Milstein catalyst #4 | | 0.050 | 160 | 55.1 | 24 | Ethylene glycol, p- Xylene glycol | $C_2$, $C_8$ | >99% | |
| PLA (cup) | Milstein catalyst #4 | | 0.133 | 160 | 55.1 | 24 | Propylene glycol | $C_3$ | >99% | |
| PPC | Milstein catalyst #2 or 4 | | 0.048 | 160 | 55.1 | 24 | Propylene glycol, methanol | $C_1$, $C_3$ | >99% | |
| PEC | Milstein catalyst #2 or 4 | | 0.026 | 160 | 55.1 | 24 | Ethylene glycol, methanol | $C_1$, $C_2$ | 91% | |
| PHB | Milstein catalyst #4 | | 0.050 | 160 | 55.1 | 24 | Butyric acid | $C_4$ | 88% | |
| P3HP | Milstein catalyst #4 | | 0.130 | 160 | 55.1 | 24 | Propionic acid | $C_3$ | 90% | |
| PET (powder) | $MoO_2/C$ | 3.23% Mo | 0.760 | 260 | 1 | 24 | Terephthalic acid | $C_8$ | 87% | 23 |
| PET (bottle) | | | 0.875 | 260 | 1 | 24 | | | 86% | |
| PET (TPA as model) | $Co/TiO_2$ | 5% | [c] | 340 | 30 | 4 | Arenes (Xylene, Toluene) | | 84% | 22 |
| PET (TPA as model) | | | | 320 | 30 | 4 | Arenes (Xylene, Toluene, p-Toluic acid, etc.) | $C_7$- $C_{16}$ | 82% | |
| PET | | | | 320 | 30 | 8 | Arenes (Xylene, Toluene, Cumene) | $C_7$-$C_{20}$ | 57% | |
| PET | | | | 320 | 30 | 24 | | $C_7$-$C_9$ | 79% | |

| | | | | | | | | | | |
|---|---|---|---|---|---|---|---|---|---|---|
| PBS | Pd/C | 5% | 0.100 | 240 | 60 | 36 | Liquids ( incl. THF) | $C_4$-$C_8$ | 79.4% (59.5% THF)[b] | [58] |
| PBS | | | | 240 | 60 | 12 | | | 86.3% (35.8% THF)[b] | |
| *n*-hexadecane | $Ru/CeO_2$ | 5% | 0.044 | 240 | 60 | 1 | Gases, Light Liquids | $C_1$-$C_{15}$ | 19% | [59] |
| Squalane | | | 0.024 | 240 | 60 | 6 | Specific liquid hydrocarbons | $C_9$-$C_{26}$ | 60% | |
| Squalane | $Ru/TiO_2$ | 5% Ru | 0.024 | 240 | 60 | 12 | Liquid alkanes | $C_9$-$C_{30}$ | 76% | [60] |
| Squalane | $Ru\text{-}VO_x/SiO_2$ | 5% Ru; 0.63% V | 0.071 | 240 | 60 | 15 | | $C_9$-$C_{30}$ | 46% | |
| Squalane | | | 0.024 | 240 | 60 | 96 | | $C_9$-$C_{19}$ | 64% | |
| *n*-hexadecane | | | 0.009 | 240 | 60 | 2 | | $C_9$-$C_{15}$ | 4% | |
| PC (pellets) | Rh/C + H-USY (Phys. mixture) | 5% (Rh on C) | 0.200 | 200 | 35 | 12 | Liquid Fuel (propane-2,2-diyldicyclohexane) | $C_{15}$ | 94.9% | [61] |
| PC (DVD disc) | | | | 200 | 35 | 12 | | | 86.9% | |

**Notes:** Distinct products (and their corresponding carbon numbers and yields) are separated by ";" as reported in their respective studies whereas those separated by "," have been reported as a single product class, PEC: polyethylene carbonate, PHB: poly(R-3-hydroxybutyric acid), PHP: poly(3-hydroxypropionic acid), PPO: poly(p-phenylene oxide). [a]$C_N$ calculated from article data ($M_n$/14). [b]Mass (wt%) yield. [c]Data not reported.

## 2.4. Mechanistic Insights from Model Compounds and Plastics Hydroconversion

A knowledge gap exists between hydroconversion of small alkanes and plastics. As PO hydroconversion typically occurs in the viscous melt phase, it likely occurs in a mass-transfer limited regime. As such, the translation of mechanistic insights from small alkane to PO hydroconversion is difficult. It is desired to elucidate the nature of active sites, reaction intermediates, chemical kinetics, and reaction pathways for PO hydroconversion, especially under reaction conditions for mechanistic understanding and informing future catalyst design. In this section, we highlight the insights from small alkane hydroconversion toward PO hydroconversion.

### 2.4.1. Model Compound Hydrogenolysis

Traditionally, hydroconversion has been focused on breaking C-X (C-C, C-S, C-O, and C-N) bonds in crude oil to make fungible fuels and chemicals.[62-67] In general, C-X bond cleavage (*e.g.*, C-O, C-C) is required to upcycle plastics. As discussed in the previous section, hydroconversion includes two distinct pathways, namely, hydrogenolysis and hydrocracking.[17,46] A detailed kinetic and mechanistic study on the hydrogenolysis for a range of alkanes ($C_2$-$C_{10}$) over metal clusters (Ir, Rh, Pt, and Ru) was reported by Iglesia and coworkers.[26,33,68-71] The hydrogenolysis reactions are structure-sensitive and were shown to have an apparent negative order with $H_2$ pressure (> 20 bar $H_2$).[72-74] This was consistent with a mechanistic picture of a rate-determining C-C bond cleavage step of a kinetically-relevant dehydrogenated surface intermediate ($C_nH_x$), formed through the C-M (metal) bonds replacing C-H bonds in the alkanes, competing with adsorbed surface hydrogen (H*).[45,63] The hydrogenolysis reaction rates therefore, depend on the surface coverage of the dehydrogenated intermediate on the catalyst surface.[75,76]

Kinetic studies showed that the hydrogenolysis rate constants for *n*-decane were eight orders of magnitude (~$10^8$) higher than for ethane (**Figure 8**).[77] The activation enthalpies ($\Delta H^{\neq}$) were found to be largely independent of the chain length and location of C-C cleavage for $C_{4+}$ *n*-alkanes.[68] Accordingly, the large difference in rate constants was attributed to the large activation entropy ($\Delta S^{\neq}$) increases with the increase in the chain length. Careful evaluation of the probable transition states (TS) indicated that the specific location of the C-C bond cleavage was suggested to depend primarily on the chain-length dependent rotational entropy of the alkyl groups connected to the carbon atoms which were bonded with the surface metal atoms, in turn showing preference for non-terminal C-C bond cleavage.[69]

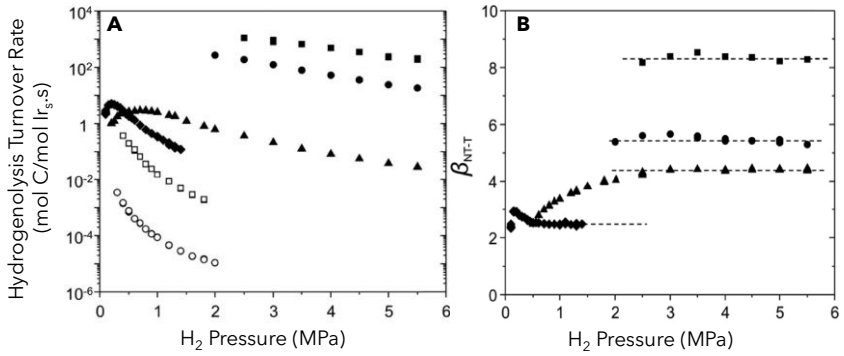


**Figure 8**. **A.** Turnover rates of alkane hydrogenolysis for ethane (○), propane (□), *n*-butane (⧫), *n*-hexane (▲), *n*-octane (●), and *n*-decane (■) as a function of $H_2$ pressure. **B.** $\beta_{NT-T}$: Ratio of turnover rates for nonterminal and terminal C−C bond hydrogenolysis normalized by the statistical occurrence of the bonds within *n*-butane (⧫), *n*-hexane (▲), *n*-octane (●), and *n*-decane (■) as a function of $H_2$ pressure. Reaction conditions: 0.7 nm Ir clusters at 20 kPa alkane, 593 K. Reprinted with permission from Flaherty *et al.*[77] Copyright 2013, American Chemical Society.

## 2.4.2. Polymer Hydrogenolysis

Consistent with small alkane hydrogenolysis, several studies on POs have reported increasing reaction rates with molecular weight.[5] Furthermore, the high selectivity to liquid hydrocarbons at low reaction times points to a preferential cleavage of non-terminal C-C bonds for POs.[24,48] Compared to small alkanes, POs have been postulated to chemisorb stronger due increased Van der Waals interactions (with a higher number of -$CH_2$ groups) with the catalyst surface.[17,68] The difference in chemical potential of POs between alkanes employed in the studies would also likely lead to stronger binding of POs.[77]

The stronger binding of PO can potentially lead to three main effects. First, the stronger interaction of PO with the catalyst surface could lead to multiple carbon-metal (C-M) bonds and non-selective C-C cleavage. In addition, multiple C-M bonds that need to be broken prior to desorption may lead to secondary C-C cleavages.[77] This is one of the likely reasons for the high methane selectivity on Ru catalysts. The influence of $VO_x$ species on Ru-$VO_x$/$SiO_2$ catalysts in reducing $CH_4$ selectivity was indeed attributed to the reduction in Ru ensembles and therefore, the reduction in non-selective C-C cleavage.[47]

Second, the stronger polymer-metal interaction may result in the apparent positive reaction order with $H_2$, particularly regarding the increasing liquid yields reported.[17,24,50] In addition, the increased $H_2$ pressure promotes hydrogenation of surface $C_nH_x$ intermediates and improves the selectivity of primary products consistent with the improved liquid alkane selectivity with an increase in $H_2$ pressure.[47]

Third, according to the Sabatier principle, overly strong or weak C-M bonds would form a very stable or weakly adsorbed polymer on the catalyst surface and consequently lower reaction rates.[45,78] Thus, a medium-strength C-M bond is desired for best performance. Ru on C, $TiO_2$, and $CeO_2$ show higher activity as compared to other metals, mirroring the trend for ethane hydrogenolysis, which is grounded in the Sabatier principle.[25,44]

### 2.4.3. Degree of Substitution in Hydrogenolysis

Next, we focus on the effect of the degree of substitution ($^1$C, $^2$C, *etc.*) on small alkanes and PO hydrogenolysis. The kinetics and mechanisms investigated from squalane and *n*-hexane hydrogenolysis on $Ru/CeO_2$ and $Ru/SiO_2$ revealed that the cleavage of $^2$C-$^2$C shows an apparent zero-order variation with $H_2$ pressure as compared to cleavage of both terminal $^2$C-$^1$C, and $^3$C-C bonds, which both show apparent negative reaction orders with $H_2$ pressure.[79] As such, a high $H_2$ pressure can lead to highly selective $^2$C-$^2$C bond cleavage and reduction in hydrogenolysis rates with higher degree of substitution (e.g., PP vs PE) on Ru catalysts. The $\Delta H^{\ddagger}$ and $\Delta S^{\ddagger}$ were found to be larger for the cleavage of $^3$C-C bonds over less substituted (*e.g.*, $^2$C-$^2$C, $^2$C-$^1$C) C-C bonds on metal clusters of Ir, Rh, Ru, and Pt.[26,68,77] As such, higher temperatures favor the cleavage of $^3$C-C bonds ($\Delta G^{\ddagger}=\Delta H^{\ddagger}-T\Delta S^{\ddagger}$), consistent with the higher temperature required to achieve selective liquid alkane formation from PP and PS hydrogenolysis.[24,26,48]

Mechanistic insights on PE hydrogenolysis were first reported on a well-defined Zr catalyst, through kinetic and DFT studies. The PE hydrogenolysis mechanism was suggested to be similar across other active metals (Pt and Ru).[27,47] In the first step, hydrogen is removed from a C-C bond, and the PE adsorbs to the active metal (M) with a C-M bond, replacing a C-H bond and releasing gaseous $H_2$. Next, hydrogenolytic cleavage breaks the C-C bond, resulting in two alkyl groups adsorbed onto the metal. Finally, both alkyl groups are desorbed and hydrogenated to form two alkanes, and a M site is regenerated. (**Figure 9**).

### 2.4.4. Hydrocracking

As compared to hydrogenolysis, in hydrocracking, the metal sites dehydrogenate the alkanes to olefins, which then interact with Brønsted acid sites that catalyze skeletal isomerization and $\beta$-scission, (*i.e.*, C-C cracking) through a carbenium ion mechanism and form two olefins.[17] Finally, the metal sites hydrogenate the smaller olefins to form alkane products, as shown in **Figure 9**. Skeletal isomerization can cause a high degree of branching in the final products. Vlachos and coworkers reported the efficacy of this mechanism in PO hydrogenolysis on Pt-based bifunctional catalyst (*e.g.*, $Pt/WO_3/ZrO_2$).[36,37] Interestingly, $Ru/WO_3/ZrO_2$ showed negligible hydrocracking activity (only hydrogenolysis), despite the presence of both metal and acid sites.[50] It

was hypothesized that Ru exhibits strong C-M metal bonds, which prevents formation of olefinic bonds that can undergo acid-catalyzed skeletal isomerization and *β*-scission, thus operating as a monofunctional catalyst.[50,75,76,80]

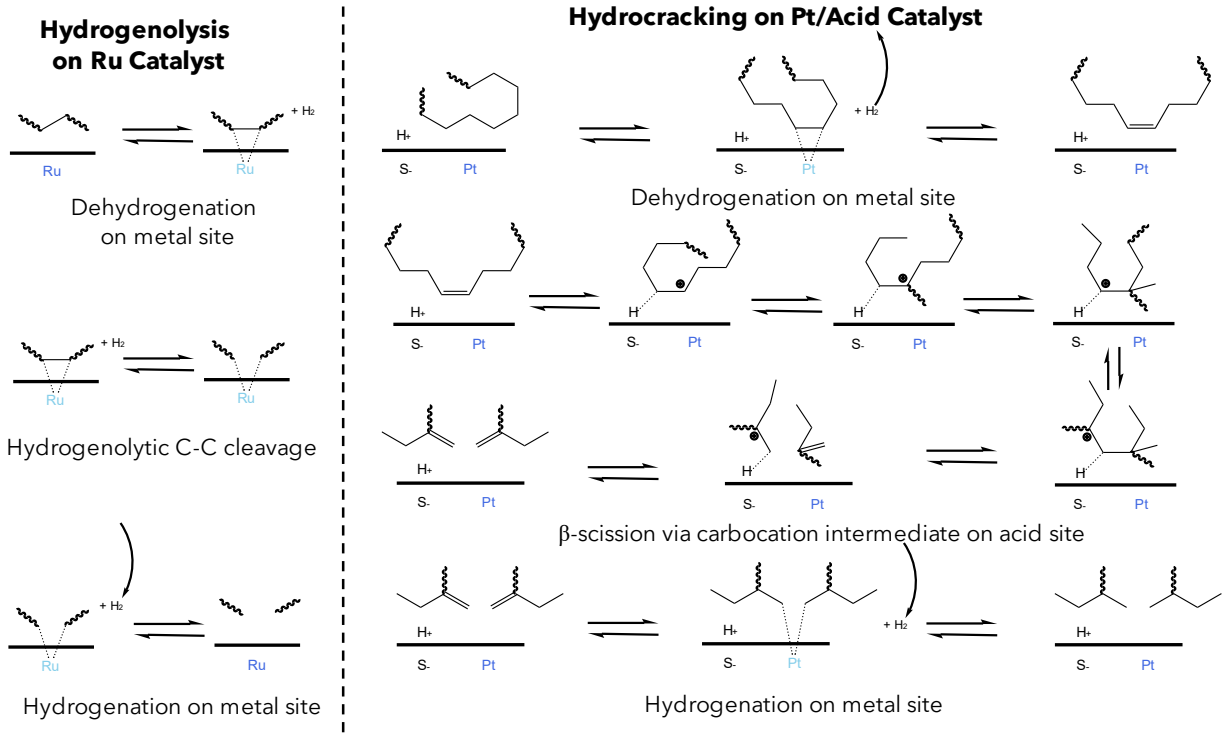


**Figure 9. Comparison of reaction mechanisms for hydrocracking and hydrogenolysis of polyolefins.** (Left) Hydrogenolysis consists of three steps; dehydrogenative adsorption of the C-C bond on the metal surface, hydrogenolytic cleavage of the C-C bond, and hydrogenative desorption leading to the formation of alkane products. (Right) Hydrocracking involves dehydrogenative adsorption of the C-C bond on the metal surface, forming an unsaturated PO followed by desorption. A proton attack on the olefinic bond forms a carbenium ion which rearranges and undergoes β-scission to form two olefins, which undergo further hydrogenation to form alkane products. The wavy bonds represent long chain alkyl groups found in PEs and the boxed metals represent supported catalyst surfaces. $H^+$ indicates a Brønsted acid site on the catalyst surface, while $S^-$ indicates the negative counterion. Pt/Ru indicate a metal site on the catalyst surface. Adapted with permission from Kots *et al.*[17] Copyright 2022, Royal Society of Chemistry.

# 3. Plastic Waste Pyrolysis

Another route for plastic waste upcycling is pyrolysis in which the long-chain polymer chains are deconstructed to gases ($C_1$-$C_5$), liquid oils that include wax and long-chain oligomers ($C_5$-$C_{20}$), and char (unreacted solid), at high temperatures (350-

1300°C) under an inert atmosphere.[81,82] This technology can produce fungible liquid products (yields upto 85 wt%) from plastic wastes. Importantly, this technology can accept a wide variety of feedstocks (*e.g.,* mixed waste, multilayer packaging), requires less pretreatment, and has an overlap with biomass valorization. We note that the pyrolysis operating temperatures are higher than those used for hydroconversion. In this section, a brief overview of plastic waste pyrolysis (PWP) is presented, emphasizing catalytic processes.

Pyrolysis can be classified by heating rate (slow, fast, and flash), heating medium (steam, vacuum, microwave, plasma, *etc.*), and catalyst use (thermal or catalytic).[82] The thermal energy breaks the carbon chains and vaporizes fragmented oligomers from the plastic surface. High heating rates and temperatures above 700°C favor gaseous products ($C_1$-$C_5$) while condensable oils and waxes are favored at milder temperatures (~500°C) and lower heating rates. To maximize liquid production, a high heating rate coupled with short residence time and rapid volatile quenching is desired.

Due to environmental and health hazards, plastics that release toxic chemicals on degradation (*e.g.,* PVC) are generally not pyrolyzed (max amount of ~ 2 wt%). Also, the pyrolysis of PET waste produces oils with lower calorific value and forms by-products (*e.g.*, CO and $CO_2$). Hence, PET is upcycled *via* other options such as hydroconversion and solvolysis.[83] Generally, POs, PS, and polyurethane (PU) make ideal feed for PWP.[84] Because of its large volume in municipal solid waste (~60%), pyrolysis of POs is extensively researched. An overview of recent works published on polymer pyrolysis is presented in Table S2.

# 3.1. Catalytic Pyrolysis

Compared to non-catalytic thermal pyrolysis, catalytic pyrolysis can significantly improve the quality of the product by narrowing its carbon distribution and improving selectivity, lowering operating temperatures, and increasing reaction rates.[84] For instance, in some cases, gas products with $C_2$-$C_4$ selectivity of up to 75% have been reported.[85,86] A variety of catalysts have been explored for catalytic pyrolysis, including, aluminosilicates (zeolites, mesoporous and amorphous silica-alumina), clay-based catalysts, metal oxides, carbonates, or carbon-based materials (*e.g.,* activated carbon).[87] A recent review was published dedicated to catalysts used in the pyrolysis of plastic wastes including operating conditions and product distributions for different types of plastic waste.[4] The relevant pyrolysis catalysts are further examined in the sections below.

## 3.1.1. Amorphous and Mesoporous Silica-Alumina Catalysts

Amorphous silica-alumina ($SiO_2$-$Al_2O_3$) catalysts have been extensively used for the pyrolysis of plastic wastes. Compared to thermal pyrolysis, amorphous $SiO_2$-$Al_2O_3$

accelerate the reaction rates and alter the product distribution. For example, while thermal pyrolysis of PS produced only styrene and dimeric products, amorphous $SiO_2$-$Al_2O_3$ favored the production of benzene and cumene.[88] However, due to the lack of a pore network, silica-alumina showed less control over product selectivity.

With regards to the nature of the active site, $SiO_2$-$Al_2O_3$ contains both Lewis- and Brønsted acid sites.[87] The increased acidity (controlled by Si/Al ratio) results in more gaseous products, while lower acidity promotes more liquid products. For instance, Sakata *et al.* evaluated HDPE pyrolysis with different types of $SiO_2$-$Al_2O_3$ catalysts: SA-1 and SA-2.[89] Unsurprisingly, a lower quantity of liquid (~50 wt%) was obtained when using the catalysts with higher acidity. In contrast, mainly liquid products (~74 wt%) were obtained using catalysts with lower acidity.[87]

Mesoporous $SiO_2$ and $SiO_2$-$Al_2O_3$ catalysts offer control over product selectivity. The ordered mesoporosity allows for improved diffusion to the acid sites, which accelerates the rate of degradation and achieves better control over product selectivity. The weak acidity of these types of catalysts inhibits secondary cracking, resulting in higher yield of liquid products. For example, liquid product selectivity (towards fuels instead of oils and wax) up to 86% for PP and 71% for PE, respectively, was reported over mesoporous $SiO_2$.[90] MCM-41 and SBA-15 were commonly investigated catalysts. The large pore size of mesoporous $SiO_2$-$Al_2O_3$ allows for improved intercalation of polymer molecules to Brønsted acid sites, displacing moderately cracked products and preventing secondary cracking.[91] These catalysts are reported to be coke-resistant due to their weak acidity. However, in the presence of heteroatoms, increased coke formation and subsequent catalyst deactivation were reported.[92]

### 3.1.2. Zeolites

Zeolites, natural, synthetic, and metal-doped (*e.g.,* Ni, Co, Mo), are the most widely used pyrolysis catalysts for POs.[4,93] They consist of three-dimensional frameworks and contain a unified structure of open pores and channels. Notably, the high acidity of zeolite catalysts enables them to be more active in cracking, with a subsequent increase in production of light olefins and a concomitant decrease in the heavy fractions.

Y-zeolite, commonly used in PE and PP pyrolysis, was reported to increase the yield of gaseous hydrocarbons. However, the presence of micropores and high acidity results in fast catalyst deactivation, and relatively large pores result in broader product distribution. The second most commonly used zeolite is MFI (silicalite-1) type ZSM-5. Its strong acidity and pore structure promotes the aromatization of intermediate products and therefore increases aromatic yields. However, this leads to coke formation and rapid catalyst deactivation. The coke formation has been mitigated in nanocrystalline zeolites that showed improved accessibility and better stability.[92] β-

Zeolite, a three-dimensional pore network with two distinct polymorph structures, favors gas products due to secondary cracking, along with the production of waxes. Naturally occurring zeolites, such as clinoptilolite and mordenite (MOR) showed moderate cracking ability and improved yields of liquid products along with higher char production.[4]

Doping is a strategy to enhance catalytic activity and improve thermal stability of zeolites. For example, transition metals such as Pd, Ni, Co, and Mo added to the zeolites can promote hydrogenation, dehydrogenation, and hydro-isomerization reactions,[4] that can tune product selectivity. Overall, zeolites are a promising material for catalytic pyrolysis; however, challenges around catalyst deactivation remain.

### 3.1.3. Other Catalysts

Clay-based materials, derived from $SiO_2$, $Al_2O_3$, and MgO, have a microporous structure and weaker acid sites compared to zeolites. Therefore, they minimize coke formation and maximize the formation of wax or diesel range products, due to a reduction in secondary cracking. Pillared clays can also include oxides of metal (*e.g.,* Fe, Zr, Ti) that influence acid site strength and distribution. They were reported to minimize side reactions and improve thermal stability.[4]

Mixed metal oxides have also shown promising results for the catalytic pyrolysis of plastics.[4] The basic nature of CaO and MgO were found to enhance the selectivity toward phenolic products from PC pyrolysis. With PO, MgO favored the production of diesel-range fuel and gaseous products. Both MgO and CaO result in a large amount of char. $ZrO_2$ and sulfated-$ZrO_2$ showed high cracking performance, albeit with rapid coke formation, due to their acidity. However, the addition of noble metals such as Pt, Ru, Ir or Rh promoted the formation of liquid products. Metal carbonates (*e.g.,* $CaCO_3$, $MgCO_3$) have also shown promise. However, their stability under the reaction conditions, remains a significant roadblock.[94,95]

Activated carbon, with its high surface area, porous structure, thermal stability, and acidic functionality, has also been used for the plastics pyrolysis. Interestingly, it was found to be an excellent choice for producing jet fuel range oils from POs. Notably, the aromatic fraction in the product increased with increasing acid strength.[96] The acid strength was tunable *via* surface functionalization with hydroxyl groups of phosphorus.

Notably, multicomponent and commercial fluidized catalytic cracking (FCC) catalysts, used in petrochemical refineries to crack heavy hydrocarbon fractions into lighter fractions, are promising for the pyrolysis of plastic waste promoting the formation of liquid products from a mixed plastic waste stream.[97] The mixture of components such as zeolites, $Al_2O_3$, $SiO_2$, and clay can together act as binders, promotors, and fillers. The components are mixed as a slurry and then spray-dried to form powder catalysts.

## 3.2. Reaction Mechanism for Catalytic Pyrolysis

A substantial amount of work has been done to develop the mechanism of catalytic pyrolysis of hydrocarbons, and there is still continuing discussion on the reaction mechanism. However, the mechanism depicted by Wojciechowski is the generally accepted mechanism for the catalytic pyrolysis of polymers. [97,98,99] In this mechanism, the chain reaction is broken down into four major steps, wherein carbenium ions play the central role (see **Figure 10** below). First, for the initiation, the feed, consisting of paraffins and/or olefins, is protonated at a pristine Brønsted acid site on the catalyst surface. The formation of surface carbenium ions from olefins is labile. Paraffins, conversely, may follow various routes to form surface carbenium. One commonly accepted route involves the initial adsorption, forming a surface carbonium ion, followed by the scission of the ion, releasing gaseous hydrogen or a shorter paraffin and leaving a carbenium ion on the surface.

After the initiation step, propagation occurs *via* a disproportionation step. Disproportionation involves the transfer of a carbon-containing moiety, or fragment, from the feed molecule to the surface carbenium ion. Alternatively, the surface carbenium ion can undergo a chain transfer step *via* β-scission, wherein a paraffin is released to the gas phase, and a smaller carbenium ion remains on the surface. Lastly, the chain reaction is terminated in a desorption step, yielding a gas phase olefin, and regenerating the Brønsted acid site.

This mechanism shown here simplistically portrays the major steps of catalytic cracking, while secondary reactions, carbonium ions, and Lewis sites can also play a role.[97-99] Typical catalysts for this mechanism, such as zeolites (HZSM-5) and silica-alumina are discussed above. Furthermore, this mechanism applies to the temperature range of 250-550°C, below the region of thermal decomposition, wherein free radical decomposition dominates.

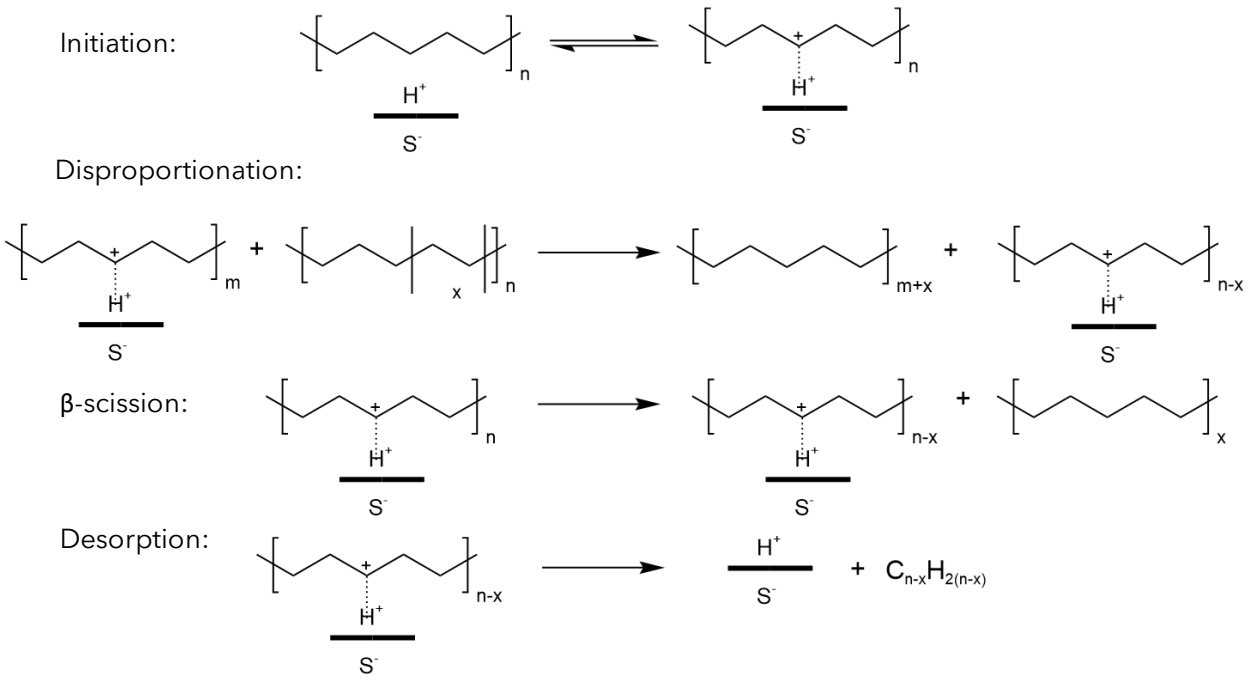


**Figure 10. Schematic for the catalytic pyrolysis of PE on Brønsted acid sites.** $H^+$ is the Brønsted acid site on the catalyst surface, and $S^-$ is the counter-anion at that site. The value of *x* can range from 0 to *n*-1. Lewis Acid sites not shown for brevity.[97,98] Adapted with permission from Zavala-Gutiérrez *et al*. Copyright 2019, American Chemical Society.

# 4. Solvent Treatment

Hydroconversion of polymers is typically conducted in the melt phase, under solvent-free conditions to avoid the susceptibility of the solvents to hydroconversion. In contrast to hydroconversion, a solvent treatment process utilizes solvents to depolymerize condensation polymers (*e.g.*, polyesters, carbonates, amides). The reaction conditions are typically milder (**see Table 2**) as compared to hydroconversion. In this section, we highlight two types of solvent treatment. First, the solvolysis route requires solvent molecules to depolymerize plastics yielding monomers or monomer derivatives at elevated temperatures (80-240°C). The monomers or their derivatives may be then subjected to secondary treatment. Second, the solvent extraction route utilizes solvents to sequentially remove certain plastics from a multi-layered plastic, or composite plastics, which can also undergo further processing.

## 4.1. Solvolysis

The solvolysis route utilizes solvent molecules to break down the polymers into monomers and/or oligomeric compounds. A variety of solvents have been reported to depolymerize post-consumer plastics, including, water, methanol, ethanol, glycols, and amines. **Figure 11** shows the typical solvolysis treatments for PET. For example, hydrolysis treatment was carried out in an acidic, basic, or neutral medium.[100] While the TPA fraction may be processed to high purity, acidic hydrolysis is expensive and adversely affects the purity of the ethylene glycol (EG) fraction.[101] Accordingly, alkaline hydrolysis of pure PET was carried out by Ügdüler *et al.* using 5 wt% NaOH in a 60:40 volumetric mixture of ethanol and water as the solvent at 80°C to give a TPA yield of 95 wt%.[102] The pure TPA can be separated by downstream filtration, following which, the solvent mixture can be distilled for solvent recovery, while the EG and any salts/additives would be left behind.

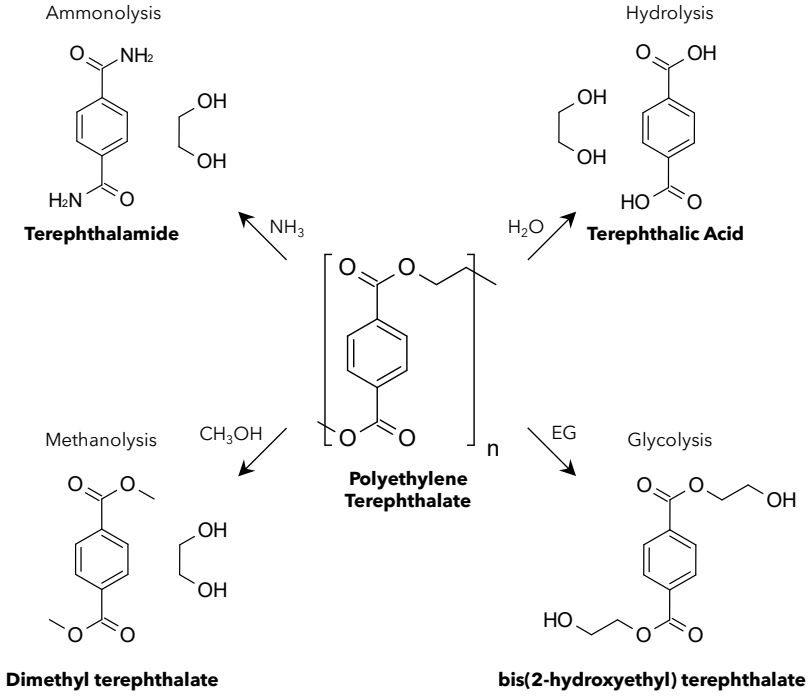


**Figure 11**. **Schematic of the solvolysis routes for PET**. The different solvents and their corresponding solvolysis products (in cyclic order: ammonia + PET → terephthalamide + EG; water + PET → terephthalic acid + EG; ethylene glycol + PET → bis(2-Hydroxyethyl) terephthalate (BHET); and methanol + PET → dimethyl terephthalate (DMT) + EG) are shown.

Ghorbantabar *et al.* recently reported a catalyst-free PET aminolysis pathway, where 85% yield of bis(2-hydroxyethylene) terephthalamide (BHETA) was achieved at 160°C using excess monoethanolamine (solvent/feed molar ratio=5) after 120 min.[103] Bäckström *et al.* further demonstrated a catalyst-free microwave-assisted aminolysis

pathway for recycling PET flakes to produce terephthalamide (TA), by using different four amines as solvents, namely, hexylamine, ethanolamine, furfurylamine, and allylamine, and obtained reasonably high TA yields of 64 wt%, 91 wt%, 82 wt%, and 61 wt%, respectively. TA was found to be promising as components for plastic film or plasticizers for PLA, exhibiting higher strain tolerance as compared to virgin PLA (as high as 20 times with 10 wt% addition of bis(furan-2-ylmethyl)terephthalamide, BTFA to PLA). A thiol-ene reaction with a tetra-functional thiol (pentaerythritol tetrakis(3-mercaptopropionate), PMP) was used to convert a diallylterephthalamide (with two functional allyl-groups formed from the aminolysis of PET with allylamine) to a resin for fabrication of films (**Figure 12**).[104]

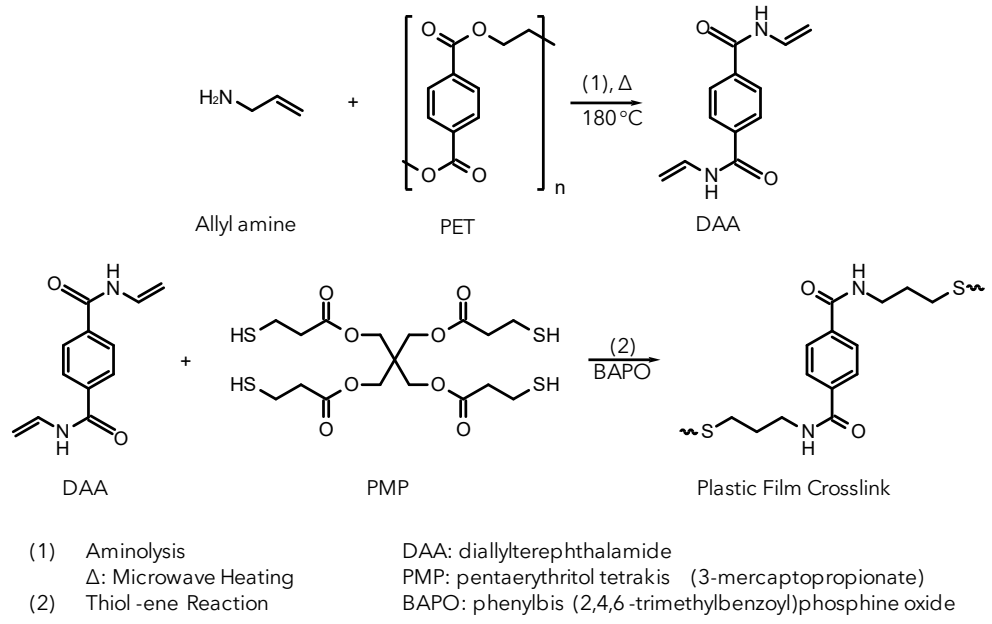


**Figure 12. Reaction scheme for the fabrication of plastic films from PET.** PET was reacted with allyl amine forming diallylterephthalamide (DAA). The DAA was then reacted with PMP, a thiol, in a thiol-ene reaction producing plastic film crosslinks. Adapted with permission from Bäckström *et al.*[104] Copyright 2021, The Authors. Published by Elsevier.

Liu *et al.* utilized a series of Lewis-basic ionic liquids (in the absence of a metal) to catalyze the alcoholysis of polycarbonate (PC). A thermally stable and recyclable (up to 6 cycles) ionic salt, 1,8-diazabicyclo[5,4,0]undec-7-enelactate ([HDBU][LAc]) was reported to catalyze methanolysis of PC at 100% conversion and a 99% yield towards the monomer bisphenol A (BPA) and dimethyl carbonate (DMC) at 120°C for 1 h (alcohol/PC molar ratio=5, catalyst/substrate molar ratio=0.008). Notably, the solvolysis rate reduced with an increase in C-number and degree of substitution among a series of higher alcohols (ethanol, *n*-propanol, *iso*-propanol, *n*-butanol, *iso*-butanol) under similar reaction conditions (**Figure 13**).[105]

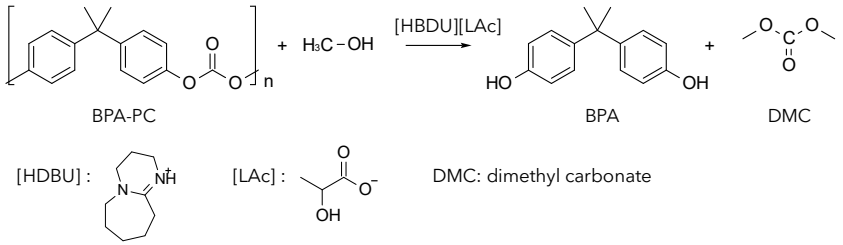


**Figure 13. Reaction scheme for the methanolysis of BPA-PC using [HDBU][LAc] as an ionic liquid catalyst.** Adapted with permission from Liu *et al*.[105] Copyright 2018, American Chemical Society.

Sardon and coworkers proposed a pathway for organocatalyzed depolymerization of PC into linear carbonates that show high ionic conductivity with potential for use as electrolytes in solid-state batteries. A series of diols (1,3-propanediol, 1,4-butanediol, and 1,5-pentanediol) were used as nucleophiles for the solvolytic deconstruction with an equimolar mixture of 1,5,7-triazabicyclo[4,4,0]de-5-ene (TBD) and methane sulfonic acid (MSA) (TBD:MSA), a protic ionic salt, as the catalyst at 160°C, to produce the monomer BPA and the carbonate-containing diols (bis(hydroxyalkyl)carbonates). The aliphatic carbonates subsequently underwent polycondensation with DMC to form linear aliphatic polycarbonates (APC) (**Figure 14**).[106] The same catalyst was also used to depolymerize BPA-PC plastics to functionalized 5 and 6-membered hetero-cyclic carbonates (along with BPA), and PET to poly(ester-amides).[107] Ethanolamine at 180°C was used to depolymerize PET, yielding 93% BHETA, which were subsequently polymerized *via* transesterification to produce poly(ester-amides).[108]

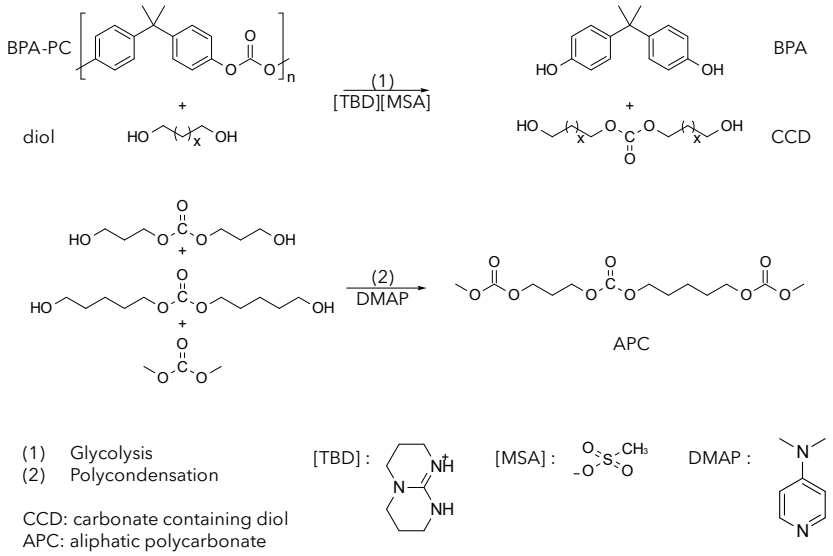


**Figure 14. Reaction scheme for the glycolysis of BPA-PC.** [TBD][MSA] was used as an ionic liquid catalyst forming carbonate-containing diols (CCD) from BPA-PC followed by the polycondensation of CCDs to form value-added aliphatic

polycarbonates. Adapted with permission from Saito *et al.*[106] Copyright 2020, Royal Society of Chemistry.

Polylactic acid, (PLA) a renewable polyester formed from the condensation polymerization of lactic acid monomers, is produced from the fermentation of corn and sugar.[109] However, under ambient conditions, PLA biodegradation can span between 12–52 weeks.[110] As such, efficient recycling and upcycling of PLA have attracted research interest.[111] Piemonte and Gironi achieved a water-soluble lactic acid yield of 95% over 2 h *via* hydrolysis of PLA at 180°C (PLA to water mass ratio = 2).[112] Ohara and coworkers compared the hydrolysis of PLA under conventional and microwave-assisted heating using a PLA/water ratio of 3:1. At 170°C, 45 wt% lactic acid yield was produced in >13 h by conventional heating whereas a comparable conversion was achieved in only 2 h through microwave-assisted heating at a greater optical purity than conventional heating (98%ee vs 94%ee).[113]

## 4.2. Tandem Solvolysis and Catalysis

Solvolysis is also employed as a first step prior to the subsequent catalytic conversion of the monomers/oligomers into value-added products. First, solvolysis breaks the polymer into its constituent monomers and/or monomer derivatives. This is followed by the catalytic upcycling of these monomeric/oligomeric compounds. One-pot strategies have been used to combine the two steps. A summary of recent works has been provided in **Table 2Table** , Table S3, and Table S4. In this section, we will outline the recent progress in the tandem process of solvolysis of single-component plastics followed by catalytic processing.

Tang *et al.* reported the selective production of $C_7$-$C_8$ cycloalkanes and aromatics *via* tandem alcoholysis of PET to form dimethyl terephthalate (DMT), followed by the hydrogenation and hydrodeoxygenation (HDO) of DMT **(Figure 15)**. Methanol, ethanol, and butanol showed PET conversion of approx. 100%, 45%, and 10%, and DMT yields of 90%, 10%, and 0%, respectively, at 180°C for 3.5 h (PET/alcohol mass ratio = 1:32). DMT was then hydrogenated to dimethyl 1,4-cyclohexanedicarboxylate (DMCD) (catalyzed by Pt/C) and finally hydrodeoxygenated to form $C_7$-$C_8$ cyclic hydrocarbons (catalyzed by oxophilic Ru-Cu/$SiO_2$).[114] In a recent study by Lu *et al.*, BTX (benzene and alkyl aromatics) were produced at substantial yields from PET in an $H_2$-free environment on Ru/$Nb_2O_5$ (220°C for 12 h in 20 bar $N_2$) in the presence of water.[115] The whole process was comprised of three tandem steps; hydrolysis of PET to form TPA, reforming of EG to generate $H_2$, and finally, decarboxylation and hydrogenolysis of TPA to form arenes (BTX).

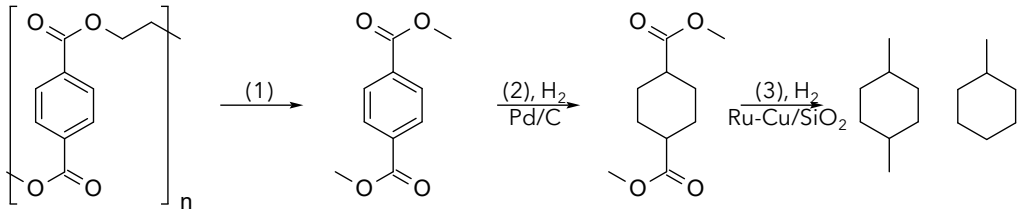


(1) Methanolysis
(2) Hydrogenation
(3) Hydrodeoxygenation

DMT: dimethyl terephthalate
DMCD: dimethyl cyclohexanedicarboxylate

**Figure 15. Reaction scheme for PET solvolysis and upcycling.** PET reacted with methanol to form dimethyl terephthalate (DMT). The DMT was hydrogenated to form dimethyl cyclohexanedicarboxylate (DMCD), which was further hydrodeoxygenated to form $C_7$-$C_8$ cyclic hydrocarbons. Adapted with permission from Tang *et al.*[114] Copyright 2019, Royal Society of Chemistry.

Li *et al.* leveraged cascade reactions to propose a one-pot system for co-processing PET and $CO_2$ into DMCD. DMCD production was accelerated by the sequential coupling of three reactions, namely, $CO_2$ hydrogenation to methanol, PET methanolysis, and DMT hydrogenation to DMCD and p-xylene. A $Cu_4Fe_1Cr_1$ catalyst performance was demonstrated to be significantly better than traditional $CO_2$ and aromatic hydrogenation catalysts such as Pd/C, CuZnAl, and Ru/C. At 240°C and 30 bar 1:1 $CO_2$+$H_2$ pressure over 12 h, a 76% EG yield and a combined 69% yield towards DMT, DMCD, and p-xylene were achieved.[116]

A recent study has explored tandem methanolysis and hydrodeoxygenation of polycarbonate to produce jet fuel range polycycloalkanes. In this process, methanolysis of PC produced BPA, which underwent HDO to form $C_{15}$ bicycloalkanes (~80% yields) in contact with Pt/C and H-Beta zeolite.[117]

Wang *et al.* reported a one-pot system for the conversion of PC that combines 1) hydrolysis, and 2) hydrogenolysis, followed by 3) dehydration/hydrogenation (**Figure 16**).[118] In a single-pot system, BPA-PC simultaneously underwent hydrolysis and hydrogenolysis over a tandem catalyst (Rh/C and H-USY zeolite) under 35 bar $H_2$ pressure and 200°C for 12 h. Thereafter, the products underwent hydrogenolysis and eventually saturation to form propane-2,2-diyldicyclohexane (PDC), suitable for jet fuel. PDC was produced at a 94.9% yield from pure PC pellets and 86.9% yield from chopped video discs (DVDs) ($CO_2$ and $CH_4$ were light gas products).

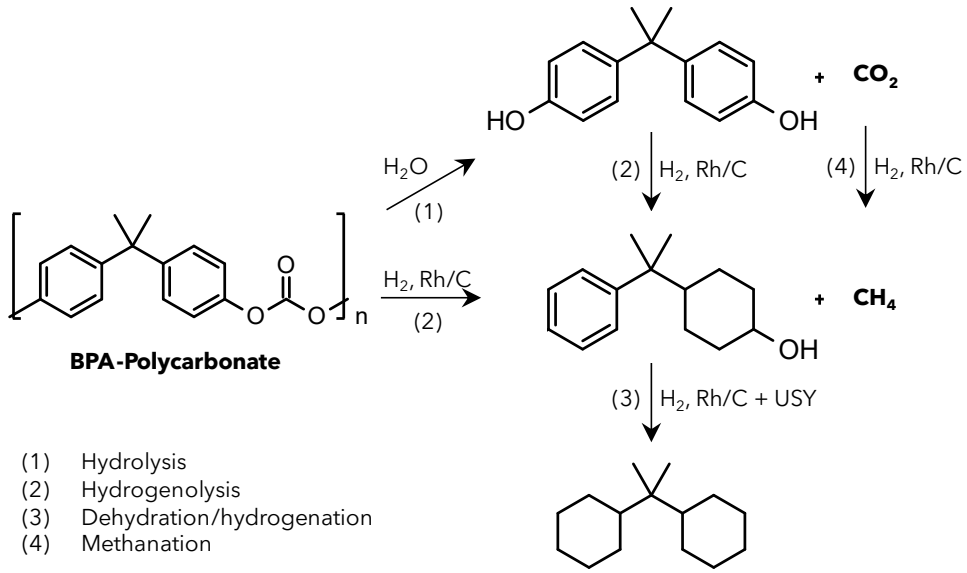


**Figure 16. Schematic for the hydrogenolysis and aqueous phase hydrodeoxygenation (APDHO) of BPA-PC.** In a single pot, BPA-PC simultaneously underwent hydrolysis (1) and hydrogenolysis (2). Both products were then hydrogenated forming propane-2,2-diyldicyclohexane (3). Adapted with permission from Wang *et al.*[118] Copyright 2021, Royal Society of Chemistry.

## 4.3. Solvent Extraction

Multilayer packaging materials are manufactured from different polymer types, which are stacked by layers, contributing layer-dependent unique properties such as, durability, thermal resistance, and hydrophobicity. Importantly, after "end-of-use", they can be cleanly sourced from industrial point sources or municipal solid wastes. To deconstruct such plastics into pure, recyclable polymers, Huber and coworkers devised a new strategy called Solvent-Targeted Recovery and Precipitation (STRAP) process.[119] Based on the specific composition of the multilayered plastic, a series of solvents were used to sequentially extract the constituent polymers. Next, the individual polymer resins were precipitated by an anti-solvent and recycled, achieving cost-competitive (compared to virgin resins) near complete recovery (**Error! Reference source not found.**).

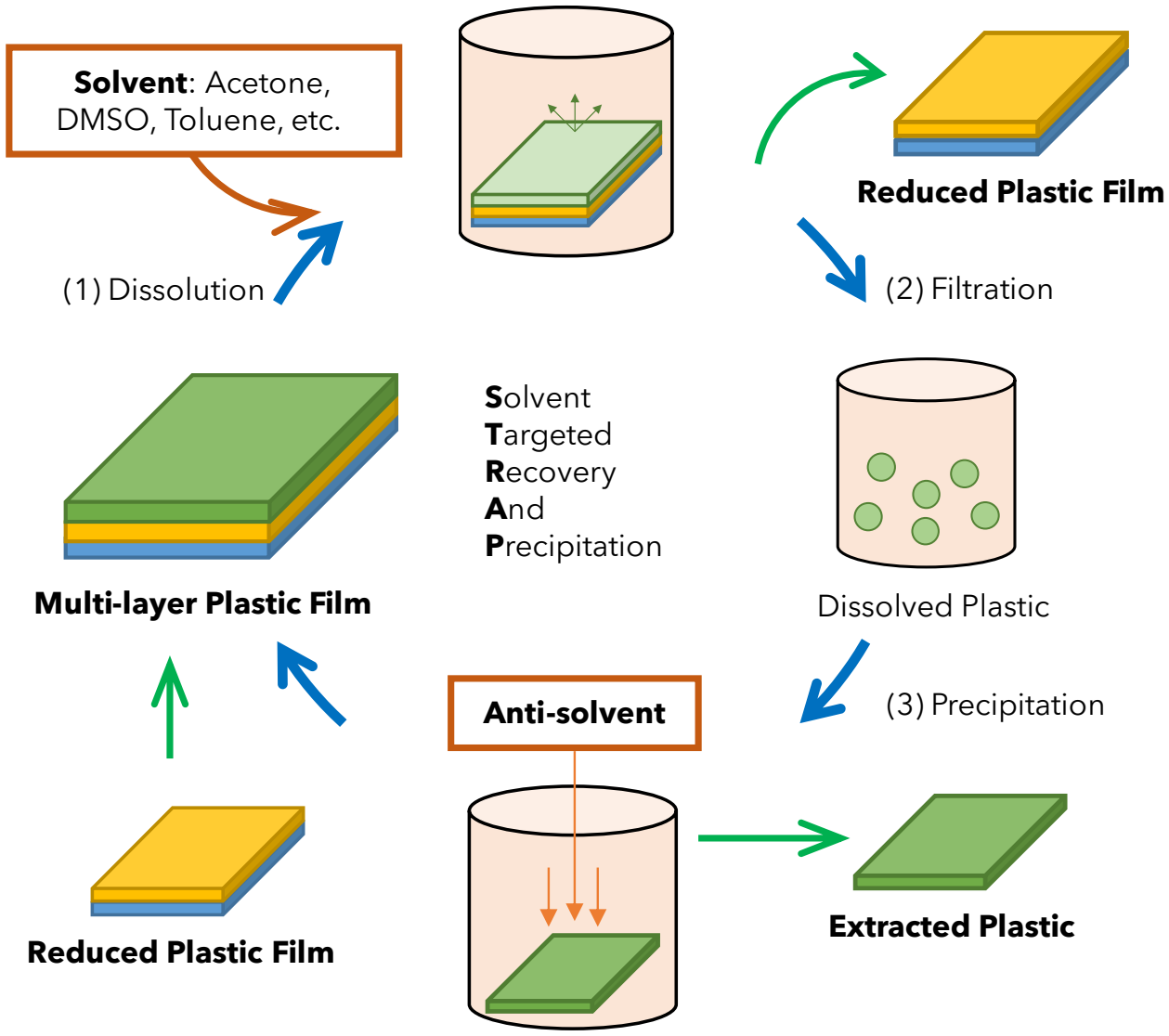


**Figure 17**. **Solvent-Targeted Recovery and Precipitation (STRAP) Process**. The optimal solvents and temperatures were determined computationally from the composition of the multilayered plastic. Sequential solvent extractions were used to extract individual polymer resins which were recovered by an antisolvent or filtration. Adapted with permission from Walker *et al.*[119] Copyright 2020, The Authors.

The optimal selection of the solvents is the key factor for an efficient STRAP process. To this end, a combination of Hansen solubility parameters (quantifying the strength of dispersion interactions, dipole-dipole interactions, and hydrogen bonding interactions between solvent and solute), molecular dynamics simulations, and combined quantum chemical-statistical mechanical approaches were used to identify appropriate solvents and their temperature-dependent solubility conditions. The process was then tested with a multilayer film of PET, ethylene vinyl alcohol (EVOH), and PE, and ~100% recovery of individual polymers was achieved. Toluene at 110°C for 4 h and dimethyl

sulfoxide (DMSO) at 95°C for 0.5 h were identified as the best solvents and process conditions for dissolving PE and EVOH, respectively, leaving isolated PET in solution. Acetone was identified as suitable anti-solvent for PE, while water was applied to both EVOH and PET.[119] Overall, the generation of a solvent library for processing multilayered plastics could enable the recycling of a wide variety of multilayered and composite plastics.

**Table 2.** Summary of recent works in the solvolysis of plastic wastes. The table highlights catalytic and non-catalytic solvolysis studies with their reaction parameters (solvent to feed ratio, catalyst feed, temperature, and duration) and the nature and yield of products.

| Substrate | Solvent | Solvent/ Feed Ratio (molar) | Catalyst | Catalyst /Feed Ratio (wt) | Temp (°C) | Time (h) | Product of Interest | Product Yield (mol%) | Ref. |
|---|---|---|---|---|---|---|---|---|---|
| PET | NaOH, Ethanol | 50 | - | - | 80 | 0.33 | disodium terephthalate | 95% [d] | 102 |
| PET | Ethanolamine | 5 | - | - | 160 | 2 | bis(2-hydroxyethyl) TA | 85% [c] | 103 |
| PET | Hexylamine | - | - | - | 180 | 0.5 [a] | dihexyl TA | 64% [c,d] | 104 |
| | Ethanolamine | | | | 200 | 0.2 [a] | bis(2-hydroxyethyl) TA | 91% [c,d] | |
| | Furfurylamine | | | | 200 | 1 [a] | bis(furan-2-ylmethyl) TA | 82% [c,d] | |
| | Allylamine | | | | 180 | 0.25 [a] | diallyl TA | 61% [c,d] | |
| PC | Methanol | 5 | [HDBU][LAc] | 0.008 (molar) | 120 | 1 | BPA | 99% | 105 |
| PC | 1,3-propanediol | 6 | TBD:MSA | 0.15 (molar) | 160 | 2.5 | BPA, bis(3-hydroxypropyl)carbonate | 99%, 98% [d] | 106 |
| | 1,4-butanediol | | | | 160 | 24 | BPA, bis(4-hydroxybutyl)carbonate | 94%, 4%, [d] | |
| | 1,5-pentanediol | | | | 160 | 0.75 | BPA, bis(5-hydroxypentyl)carbonate | 99%, 99% [d] | |
| PC | Ethylene glycol | 6 | TBD:MSA | 0.15 (molar) | 90 | 4 | Ethylene carbonate | 83% | 107 |
| | Ethylene diamine | | | | | 0.1 | Imidazolidine-2-thione | 96% | |
| | Ethylene dithiol | 3 | | | | 0.5 | 1,3-dithiolane-2-thione | 92% | |
| | Glycerol | | | | 160 | 2 | 4-(Hydroxymethyl)-1,3-dioxolan-2-one | 90% | |
| PET | Ethanolamine | 20 | TBD:MSA | 0.10 (molar) | 180 | 0.15 | bis(2-hydroxyethyl) TA | 93% | 108 |
| | 2,2-Amino(ethoxy) ethanol | | | | | 0.5 | bis(2-(2-hydroxyethyl)ethyl) TA | 92% | |
| PLA | Water | 2 (wt) | - | - | 160, 180 | 2 | Lactic acid | >95% | 112 |
| PLA | Water | 0.33 (wt) | - | - | 170 | 13.3 | Lactic acid | 45% [c] | 113 |
| | | | | | 170 | 2 [a] | | 45% [c] | |
| PET | Methanol | 32 (wt) | - | - | 200 | 3.5 | DMT | 97% [d] | 114 |
| PET | Water | 75 (wt) | $Ru/Nb_2O_5$ | 1 | 220 | 12 | BTX (benzene, toluene, xylene) | 91% | 115 |
| PET | Dioxane; Methanol ($CO_2$+$H_2$) [b] | 200 (wt); | $Cu_4Fe_1Cr_1$ | 1 | 240 | 12 | Ethylene Glycol, | 75.5% [d], 68.5% [d] | 116 |

| | | | | | | | | | |
|---|---|---|---|---|---|---|---|---|---|
| | | 14 bar $CO_2$ +14 bar $H_2$ | | | | | DMT and derivatives (directly hydrogenated) | | |
| PC | Methanol | 32 (wt) | - | - | 180 | 3 | BPA | ~90% | [117] |
| PC pellets | Water | 40 (wt) | Rh/C+H-USY | 0.2 | 200 | 12 | BPA (directly hydrodeoxygenated) | - | [118] |
| PC (DVD disc) | | | | | 200 | 12 | | | |
| PET | Ethylene glycol | 2 (wt) | $Ti(OBu)_4$ | 0.005 | 220 | 4 | Glycolized (lower $M_w$) PET | - | [120] |

**Notes:** [a]Heating by microwave irradiation, [b]Methanol is produced *in-situ* by $CO_2$ hydrogenation, TA: terephthalamide, TBD: 1,5,7-triazabicyclo[4,4,0]de-5-ene, MSA: methane sulfonic acid, DMT: dimethyl terephthalate, BPA: bisphenol-A, [c]Mass (wt%) yield, [d]Theoretical yield

# 5. Other Catalytic Upcycling Processes

In this section, we outline a number of catalytic approaches to upcycle plastics, namely, olefin-mediated cross alkane metathesis, functionalization, and tandem oxidative depolymerization followed by electro- and photocatalysis.

## 5.1. Olefin-Mediated Cross Alkane Metathesis

While hydroconversion of PEs may lead to a mixture of linear alkanes, branched alkanes, and aromatics, olefin-mediated cross-alkane metathesis was found to be selective for a mixture of linear alkanes in the absence of $H_2$ (**Figure 18**). In this pathway, the PEs and the short alkanes first undergo dehydrogenation to form olefins. Next, the resulting olefinic C=C bond in the PE and the short alkane undergo cross-metathesis to form two new lighter olefins. Finally, the resulting olefins undergo hydrogenation to form saturated alkanes.[121-123] The use of low-cost and recyclable *n*-alkanes in excess, relative to PE, reduces the number of redundant metathesis reactions between two PE chains (which would not result in the breakdown of PE).

Jia *et al.* used a γ-$Al_2O_3$-supported, "pincer"-ligated Ir-complex, ($^{t\text{-}Bu}$PCP)Ir$H_2$, and $Re_2O_7$/γ-$Al_2O_3$ for alkane dehydrogenation and olefin metathesis, respectively, which facilitated the breakdown of PE. Specifically, HDPE ($M_w$=3,350, PDI=1.6) and excess *n*-hexane underwent cross alkane metathesis at 150°C in an inert argon environment for 72 h to produce 56 wt% liquid *n*-alkane oil yield, about half being in the diesel range. The wax products showed a significant reduction in molecular weight compared to the parent PE ($M_w$=680, PDI=1.4).[123] Olefin metathesis of internal C=C bonds was shown to increase the oil yields to 98% on a similar alumina supported ($^{t\text{-}Bu}$POCOP)Ir complex, which formed internal C=C bonds. For a wide range of PEs (except for LDPE) with $M_W$ ranging from thousands to millions and dispersion values up to 13, ($^{t\text{-}Bu}$POCOP)Ir formed wax products with a $M_W$ less than 1000 and a narrow dispersion (PDI~1.3). Importantly, both the supported Ir and olefin metathesis catalysts showed tolerance to polymer stabilizers and plasticizers present in commercial PEs, showing their efficacy for the upgrading of waste PE bottles, films, and bags.

In another study, Beckham and coworkers used a mixture of SnPt/γ-$Al_2O_3$ (dehydrogenation/hydrogenation catalyst) and $Re_2O_7$/γ-$Al_2O_3$ (olefin-metathesis catalyst) for olefin-mediated cross-alkane metathesis of PE with *n*-pentane. This system produced a wide distribution of *n*-alkane products from a model linear $C_{20}$ alkane, *n*-eicosane, and a linear PE (representative of HDPE). A decrease in molecular weight by 73% was observed for PE at 200°C in 15 h with a total liquid alkane yield of 99 wt%.[124]

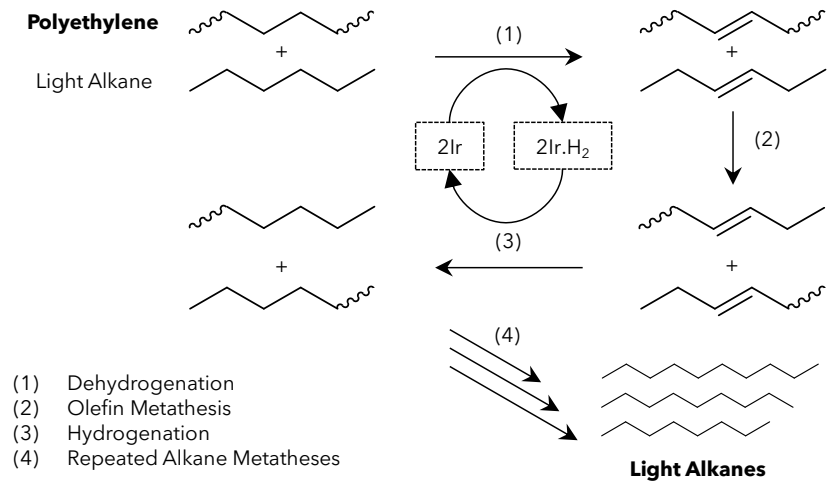


**Figure 18**. **Schematic of Olefin Mediated Cross-Alkane Metathesis (CAM)**. When reacted with a light alkane, the PE and the light alkane first undergo dehydrogenative adsorption/desorption forming unsaturated alkanes. The pair is then crossed *via* the olefin metathesis mechanism forming asymmetric unsaturated olefins. These are then hydrogenated forming lower alkanes. The sequential metathesis reactions lead to the production of liquid fuels (linear alkanes) from PE using excess light alkanes. The wavy bonds represent long chain alkyl groups. Adapted with permission from Jia *et al.*[123] Copyright 2016, The Authors.

## 5.2. Functionalization

Functionalization of polymers is another route to upcycle plastics wherein functional groups with specific physical and chemical properties can be attached to the hydrocarbon backbone. For instance, vitrimers form permanent dynamic covalent networks during reactive extrusion and combine the properties of both thermoplastics and thermosets. The cross-linking is a single, thermally activated process and therefore has a single characteristic rate. While cooling, the network is frozen, thereby fixing the physical properties. Importantly, they behave like viscoelastic fluids at high temperatures, allowing reprocessing and making them amenable for multi-use.[125,126,127]

Kar *et al.* reported a vitrimer synthesis through the reactive extrusion of PP and HDPE packaging at 180°C and 100 rpm (**Figure 19**).[125] Moreover, this exchange was compatible with additives or contaminants. During the extrusion process, the POs were functionalized with maleic anhydride (MA) along with dicumyl peroxide (DCP), which was added as a free radical initiator. After 10 min, graft copolymers (MA-g-POs) were formed. Subsequently, a di-epoxy crosslinker (DGEBA) and catalyst ($Zn(acac)_2$) were introduced, inducing transesterification between the hydroxyl groups and ester groups of DGEBA and the grafted polymer. Wang *et al.* upcycled post-consumer LDPE plastic bags to covalent adaptable networks (CANs) *via* the transesterification reaction with MA using a bio-based crosslinker (butanediol) in a twin-screw extruder.[61]

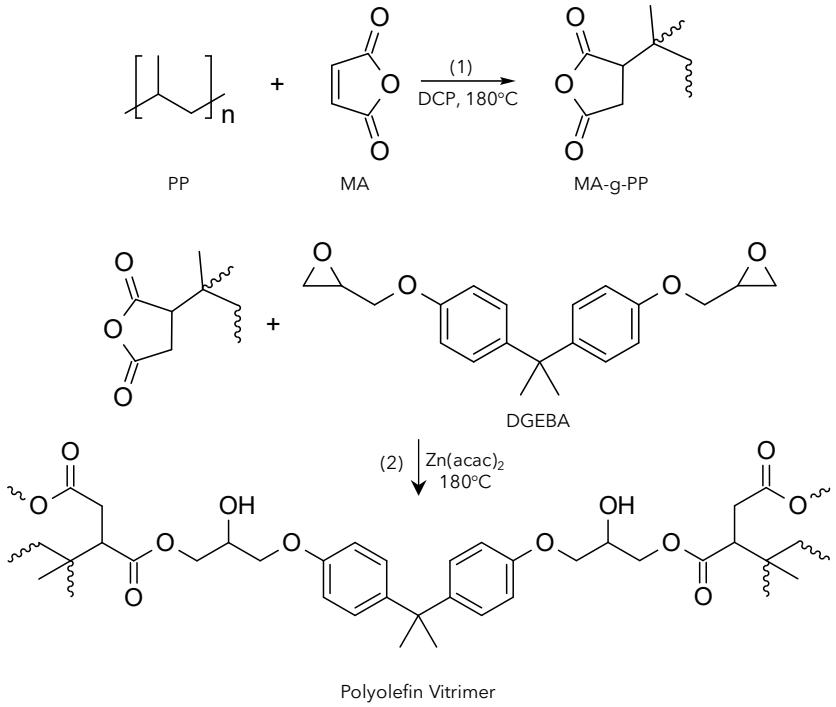


**Figure 19. Reaction scheme for the functionalization of PP into a vitrimer.** Polypropylene (PP) was reacted with maleic anhydride in presence of a free radical initiator to produce the polypropylene-maleic anhydride graft copolymer. The copolymer was then cured with epoxy to form the polyolefin vitrimer. Adapted with permission from Kar *et al.*[125] Copyright 2020, Royal Society of Chemistry.

Hartwig and coworkers identified an organometallic, polyfluorinated, ruthenium-porphyrin catalyst (high-valent Ru-oxo species) to oxidize the strong C-H bonds in PEs to hydroxyl and ketonic groups.[128] This process used 2,6-dichloropyridine *n*-oxide in dichloroethane at 120°C to selectively functionalize commodity PEs and distinctly impart adhesive properties to the polymers at 48-59% yields. This was achieved without polymer chain cleavage, overoxidation, or incorporation of chlorine in the framework.[128,129] Interestingly, even at a low mol% level of functionalization, the functionalized PEs adhere strongly to metals and POs.

Rorrer *et al.* proposed a method to upcycle waste PET to fiber-reinforced plastics (FRP) by combining deconstructed PET with renewably sourced monomers **(Figure 20)**.[120] First, PET was glycolyzed with linear diols (ethylene glycol or 1,4-butanediol) and Ti-butoxide (TiOBu) as the catalyst. Next, the glycolyzed PET was reacted to produce unsaturated polyester or diacylic polymers *via* melt blending of the deconstructed PET with olefinic diacids (malate, fumarate, and *cis,cis* and *trans,trans*

isomers of dimethyl muconate) or methacrylic/acrylic acid, over the same transesterification catalyst. These polymers were then dissolved in a reactive diluent with a free radical initiator to form a resin. The FRPs were shown to have comparable properties as virgin PET, and were found to be potentially cheaper, more energy efficient, and release less emissions than both petroleum-based FRPs and completely recycled PET.[120] Together, these findings show interesting approaches to upgrade waste plastics into "smarter" and "functional" materials.[120]

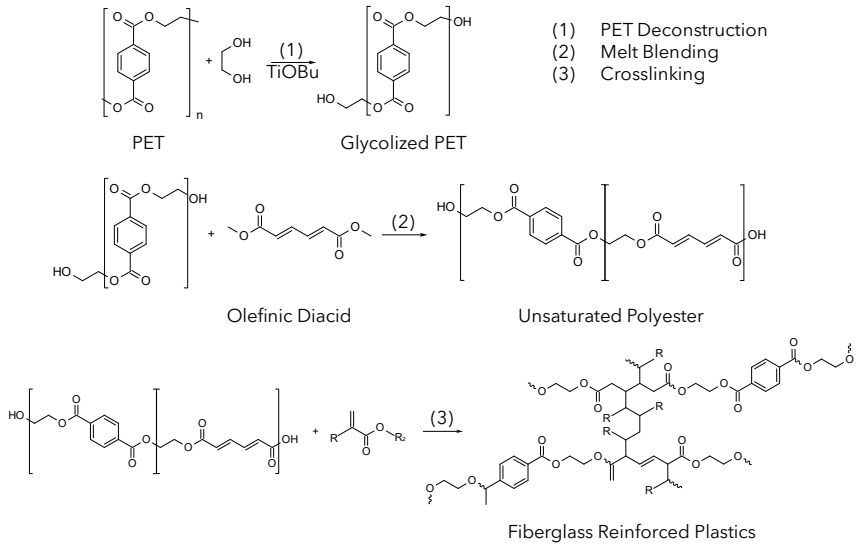


**Figure 20. Reaction scheme for the upcycling of PET waste into Fiberglass Reinforced Plastics (FRP).** PET was first deconstructed *via* glycolysis. The glycolyzed PET was reacted with olefinic diacids in a melt blending process to produce unsaturated polyester which was further cross-linked with esters forming fiber reinforced plastics. Adapted with permission from Rorrer *et al.*[120] Copyright 2019, Elsevier.

## 5.3. Tandem Oxidative Depolymerization and Photocatalysis/Electrocatalysis

Reisner and workers utilized oxidative depolymerization of PE ($M_W$=102,920, PDI=12.4) using dilute nitric acid (6 wt%) to produce dicarboxylic acids (succinic and glutaric acid) at 40% acid yields at 180°C for 4 h. This was coupled with electrocatalytic and photocatalytic decarboxylation to produce gaseous products. The oxidative/photocatalytic route produced ethane and propane (1% yield) produced using $Pt/TiO_2$ or carbon nitride as the photocatalyst, and the oxidative/electrocatalytic route produced ethylene and propylene (7.6% hydrocarbon yield) with carbon electrodes as electrocatalyst. $H_2$ and $CO_2$ were the major gaseous byproducts.[130]

# 6. Challenges and Opportunities

As outlined above, the field of catalytic upcycling and recycling has recently made significant strides towards creating a circular economy. However, significant challenges and opportunities still remain, which are outlined in this section.

## 6.1. Reporting Comparable Catalysis Data

As seen in the previous sections, the results obtained by various experimental and analytical methods cannot be easily compared. First, the polymers were typically characterized by several parameters, with molecular weight (number-average/weight-average) and polydispersity index (PDI) giving an important depiction of polymer size. Understanding the initial size and structure of the polymer is crucial to ascertaining the reaction rate and degree of depolymerization. A standard analytical technique, such as gel permeation chromatography (GPC), may be applied to characterize the deconstruction of plastics. To inform catalyst and reactor design, accurate quantification and assessment of products are also necessary. When liquid products are important, gas chromatography (GC) can be a more precise analytical technique compared to GPC. Yield data has further discrepancies, primarily regarding a lack of clarity on whether molar or mass yield is reported. Herein, a diligent effort has been made to compare the results, but more clarity on the methods, equations, results, and data is needed to improve coherency in the scientific community.

Reaction conditions, such as pressure, temperature, and reaction time, in addition to metal loading information, are often reported. However, information on the catalyst-to-feed ratio is not uniform. In this work, the mass ratio has been reported wherever available, to provide a reasonable metric for comparison. Another important metric is the catalyst- to-feed ratio in terms of moles of active metal (or acid sites) to the number of carbon moles in the polymer, which is often not reported. Overall, consistency and clarity of reported data will aid the community in moving forward.

## 6.2. Reaction Conditions

Optimization of reaction conditions such as temperature and pressure are a key objective of catalytic processes. A reduction in temperature from operating at 500-800°C to a level around 200°C has several implications including plant economics, lower heating utility requirements, lower probability of thermal runaways, and greater catalyst lifetime. A reduction in operating pressure can contribute to mitigating safety concerns. Specifically, high-pressure systems would generally require more robust process equipment and pressure safety mechanisms. As such, the catalyst processes outlined above already demonstrate improved reaction conditions, while also leaving ample room for further improvement to achieve techno-economic feasibility.

As PO hydroconversion likely occurs under a mass-transfer limited regime, the use of model compounds would be a useful tool to elucidate a complete mechanistic picture under a kinetically-controlled regime. Further, solvents that do not undergo hydroconversion are crucial to reducing mass-transfer limitations. As recently observed for several chemical transformations relevant to biomass transformation,[131,132] the effect of the solvent and the condensed-phase towards reaction kinetics and mechanism needs to be enumerated and elucidated to design optimal systems.

## 6.3. Catalyst Design, Characterization and Modeling

Beyond specificity, catalyst lifetime is also crucial to achieving process sustainability. The optimized performance can be achieved by studying coke-formation mechanisms.[133] The potential for catalyst regeneration and recyclability needs further study, as this would further promote process feasibility.

*Operando* spectroscopy, including infrared spectroscopy (IR), X-ray absorption (XAS), X-ray photoelectron spectroscopy (XPS), can reveal important insights into the nature of active sites, formation of reaction intermediates, mechanisms of the polymer degradation, and the deactivation mechanisms, under reaction conditions. However, these techniques will presumably be carried out with model compounds in the gas/vapor phase. While they provide an opportunity to study light alkane hydrogenolysis to supplement our mechanistic understandings, challenges would remain to translate these findings for the liquid-phase plastic upcycling reactions. Therefore, modeling tools such as *ab initio* DFT, Molecular Dynamics (MD), and Kinetic Monte Carlo (KMC) simulations could provide important insights into the reaction mechanisms.

## 6.4. Product Selectivity and Yield

Product streams with high yields and selectivities carry higher monetary value than mixed products, which require downstream separations. While catalytic upcycling of plastics has been shown to synthesize valuable products, the selectivity and yield remain a significant challenge. The upcycling of any polymer substrate produces a spectrum of compounds with regards to their molecular weights, isomers, and phases. For instance, diesel fuels have an average carbon number of $C_{12}$ with the hydrocarbons ranging from $C_{10}$-$C_{15}$.[134] Although some of the processes discussed above are suited toward diesel or gasoline products, further work is needed to improve selectivity, narrow the range of products generated, and improve economic viability.

While high product selectivity is desirable, the catalysts also need to be versatile for mixed feedstocks. Catalysts are currently being designed for substrate specificity. As

such, highly specific catalysts cannot effectively convert mixed post-consumer plastic streams.

## 6.5. Process Design

Process design for upcycling plastics depends largely on the nature of the feed. For instance, hydroconversion was reported to be efficient for converting POs and polyesters, while pyrolysis could be an easier option for upcycling mixed polymers. Further, solvolysis and solvent-extraction proved to be efficient for upcycling condensation polymers and composite plastic materials, respectively.

To overcome these seemingly contradicting process criteria, several approaches could be applied. Sorting feedstock based on primary functional groups of the monomers (*i.e.*, POs, aromatic polyesters, polyvinyls, *etc.*) would enable product selectivity, but this poses additional logistical challenges. Alternatively, versatile catalytic processes may handle mixed streams. Series reactors with discrete catalyst beds may be applied to sequentially process the mixed substrate, as shown in **Figure 21**. In addition, solvent-assisted separation of a mixed plastic feed can be done before the catalytic reaction. A solvent extraction scheme, such as the STRAP process[119] would be followed by parallelly converting the extracted products. The products can then be blended or processed further (**Figure 21**). A careful balance must be struck between reaction conditions and downstream/upstream separation techniques.

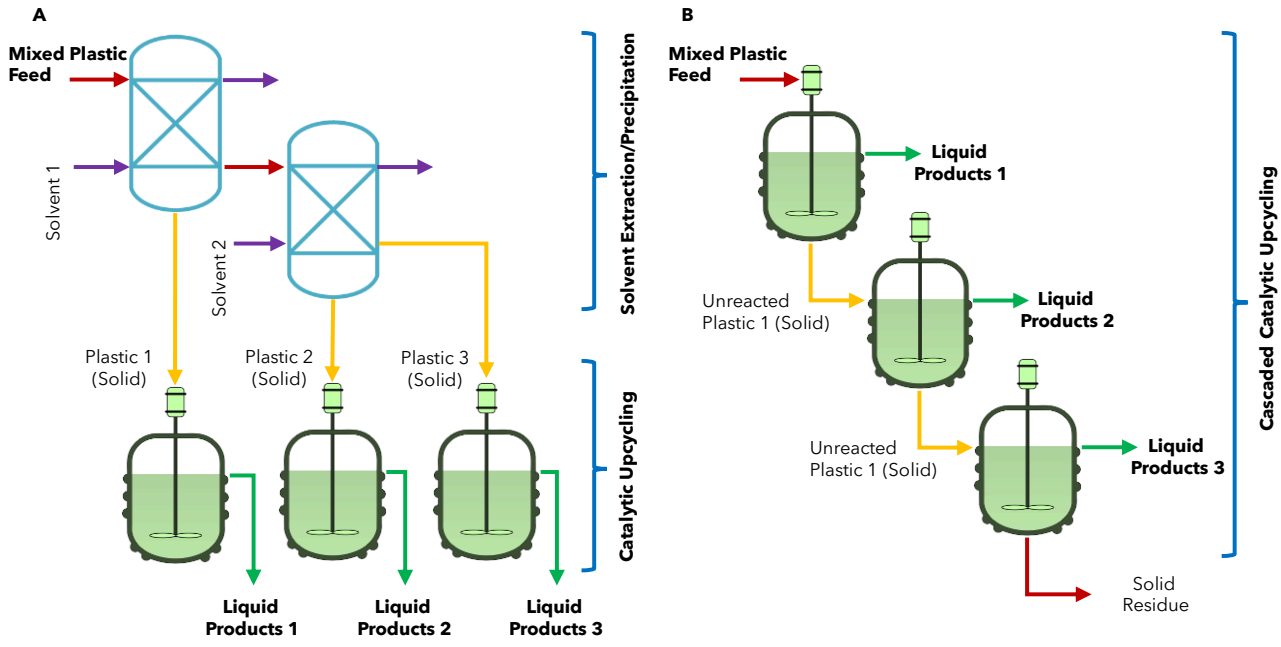


**Figure 21**. **Proposed plastic upcycling processes. A**. Upstream separation of a mixed plastic feed by solvent extraction and precipitation (such as the STRAP process)

followed by parallel catalytic upcycling and **B**. Cascaded catalytic upcycling of mixed plastic feed using a series of substrate-specific catalysts.

# 7. Conclusions and Outlook

Creating a circular plastics economy is crucial to achieving environmental sustainability. Despite worldwide efforts to "reduce, reuse, and recycle" plastics, their production still overwhelmingly eclipses their recycling. The last few years have only worsened this problem with the sudden surge in the use of "single-use" plastic products due to the COVID-19 pandemic. As things stand, catalytic hydroconversion and solvent-based approaches show promise in creating a pathway towards a circular plastics economy. Further, pyrolysis is a mature technology to convert plastics to fungible products, albeit under harsher conditions than hydroconversion and solvent-based approaches. Addressing challenges, such as milder reaction conditions, robust catalyst design, selective product yields, and, critically, feedstock versatility, must be addressed to reach the techno-economic feasibility needed to make a circular economy a reality.

**Author contributions.** M.S, S.B, and R.H. ideated and outlined the manuscript. M.A., W.M., and W.M. contributed to the pyrolysis section. S.B., R.H, F.M., and M.S. contributed the figures and tables in the manuscript. All authors contributed to editing the manuscript.

**Acknowledgments.** We are grateful to the Artie McFerrin Department of Chemical Engineering at Texas A&M University, the College of Engineering, Dr. Mark Barteau, and the Provost for their financial support. This work was funded by Texas A&M University (TAMU), Texas A&M Engineering Experiment Station (TEES), and the Governor's University Research Initiative (GURI). M.A., W.M., and W.M. acknowledge financial support by Responsive Research Grants provided by Texas A&M University at Qatar.

**Conflict of Interest.** The authors declare no conflict of interest.

**Supplemental Information description.** Additional tables, Table S1-S4, referenced in the main text, are included in the supplementary information.

# *References*


1. Rahimi, A., and García, J.M. (2017). Chemical recycling of waste plastics for new materials production. Nat. Rev. Chem. *1*, 0046. 10.1038/s41570-017-0046.
2. Geyer, R., Jambeck, J.R., and Law, K.L. (2017). Production, use, and fate of all plastics ever made. Sci. Adv. *3*, e1700782. doi:10.1126/sciadv.1700782.
3. Jambeck, J.R., Geyer, R., Wilcox, C., Siegler, T.R., Perryman, M., Andrady, A., Narayan, R., and Law, K.L. (2015). Marine pollution. Plastic waste inputs from land into the ocean. Science *347*, 768-771. 10.1126/science.1260352.
4. Mark, L.O., Cendejas, M.C., and Hermans, I. (2020). The Use of Heterogeneous Catalysis in the Chemical Valorization of Plastic Waste. ChemSusChem *13*, 5808-5836. 10.1002/cssc.202001905.
5. Celik, G., Kennedy, R.M., Hackler, R.A., Ferrandon, M., Tennakoon, A., Patnaik, S., LaPointe, A.M., Ammal, S.C., Heyden, A., Perras, F.A., et al. (2019). Upcycling Single-Use Polyethylene into High-Quality Liquid Products. ACS Cent Sci *5*, 1795-1803. 10.1021/acscentsci.9b00722.
6. Wang, C.Y., Liu, Y., Chen, W.Q., Zhu, B., Qu, S., and Xu, M. (2021). Critical review of global plastics stock and flow data. J. Ind. Ecol. *25*, 1300-1317. 10.1111/jiec.13125.
7. Chamas, A., Moon, H., Zheng, J., Qiu, Y., Tabassum, T., Jang, J.H., Abu-Omar, M., Scott, S.L., and Suh, S. (2020). Degradation Rates of Plastics in the Environment. ACS Sustain. Chem. Eng. *8*, 3494-3511. 10.1021/acssuschemeng.9b06635.
8. Zhang, F., Zeng, M., Yappert, R.D., Sun, J., Lee, Y.H., LaPointe, A.M., Peters, B., Abu-Omar, M.M., and Scott, S.L. (2020). Polyethylene upcycling to long-chain alkylaromatics by tandem hydrogenolysis/aromatization. Science *370*, 437-441. 10.1126/science.abc5441.
9. Law, K.L. (2017). Plastics in the Marine Environment. In ANNUAL REVIEW OF MARINE SCIENCE, VOL 9, pp. 205-229. 10.1146/annurev-marine-010816-060409.
10. Cozar, A., Echevarria, F., Gonzalez-Gordillo, J.I., Irigoien, X., Ubeda, B., Hernandez-Leon, S., Palma, A.T., Navarro, S., Garcia-de-Lomas, J., Ruiz, A., et al. (2014). Plastic debris in the open ocean. P Natl Acad Sci USA *111*, 10239-10244. 10.1073/pnas.1314705111.
11. Belden, E.R., Kazantzis, N.K., Reddy, C.M., Kite-Powell, H., Timko, M.T., Italiani, E., and Herschbach, D.R. (2021). Thermodynamic feasibility of shipboard conversion of marine plastics to blue diesel for self-powered ocean cleanup. P Natl Acad Sci USA *118*. 10.1073/pnas.2107250118.
12. Astrup, T., Fruergaard, T., and Christensen, T.H. (2009). Recycling of plastic: accounting of greenhouse gases and global warming contributions. Waste Manag Res *27*, 763-772. 10.1177/0734242X09345868.

13. Zhao, X., Korey, M., Li, K., Copenhaver, K., Tekinalp, H., Celik, S., Kalaitzidou, K., Ruan, R., Ragauskas, A.J., and Ozcan, S. (2022). Plastic waste upcycling toward a circular economy. Chem. Eng. J. *428*. 10.1016/j.cej.2021.131928.
14. Schyns, Z.O.G., and Shaver, M.P. (2021). Mechanical Recycling of Packaging Plastics: A Review. Macromol. Rapid Commun. *42*, e2000415. 10.1002/marc.202000415.
15. Chen, X., Wang, Y., and Zhang, L. (2021). Recent Progress in the Chemical Upcycling of Plastic Wastes. ChemSusChem *14*, 4137-4151. 10.1002/cssc.202100868.
16. Panda, A.K., Singh, R.K., and Mishra, D.K. (2010). Thermolysis of waste plastics to liquid fuel A suitable method for plastic waste management and manufacture of value added products-A world prospective. Renew. Sust. Energ. Rev. *14*, 233-248. 10.1016/j.rser.2009.07.005.
17. Kots, P.A., Vance, B.C., and Vlachos, D.G. (2022). Polyolefin plastic waste hydroconversion to fuels, lubricants, and waxes: a comparative study. React. Chem. Eng. *7*, 41-54. 10.1039/d1re00447f.
18. Infantesmolina, A., Meridarobles, J., Rodriguezcastellon, E., Pawelec, B., Fierro, J., and Jimenezlopez, A. (2005). Catalysts based on Co/zirconium doped mesoporous silica MSU for the hydrogenation and hydrogenolysis/hydrocracking of tetralin. Appl. Catal., A *286*, 239-248. 10.1016/j.apcata.2005.03.022.
19. Weitkamp, J. (2012). Catalytic Hydrocracking—Mechanisms and Versatility of the Process. ChemCatChem *4*, 292-306. 10.1002/cctc.201100315.
20. IEA (2020). Production of key thermoplastics, 1980-2050. https://www.iea.org/data-and-statistics/charts/production-of-key-thermoplastics-1980-2050.
21. Dufaud, V., and Basset, J.M. (1998). Catalytic Hydrogenolysis at Low Temperature and Pressure of Polyethylene and Polypropylene to Diesels or Lower Alkanes by a Zirconium Hydride Supported on Silica-Alumina: A Step Toward Polyolefin Degradation by the Microscopic Reverse of Ziegler-Natta Polymerization. Angew Chem Int Ed Engl *37*, 806-810. 10.1002/(SICI)1521-3773(19980403)37:6<806::AID-ANIE806>3.0.CO;2-6.
22. Hongkailers, S., Jing, Y., Wang, Y., Hinchiranan, N., and Yan, N. (2021). Recovery of Arenes from Polyethylene Terephthalate (PET) over a Co/TiO2 Catalyst. ChemSusChem *14*, 4330-4339. 10.1002/cssc.202100956.
23. Kratish, Y., Li, J., Liu, S., Gao, Y., and Marks, T.J. (2020). Polyethylene Terephthalate Deconstruction Catalyzed by a Carbon-Supported Single-Site Molybdenum-Dioxo Complex. Angew Chem Int Ed Engl *59*, 19857-19861. 10.1002/anie.202007423.
24. Rorrer, J.E., Beckham, G.T., and Roman-Leshkov, Y. (2021). Conversion of Polyolefin Waste to Liquid Alkanes with Ru-Based Catalysts under Mild Conditions. JACS Au *1*, 8-12. 10.1021/jacsau.0c00041.

25. Almithn, A., and Hibbitts, D. (2019). Comparing Rate and Mechanism of Ethane Hydrogenolysis on Transition-Metal Catalysts. J. Phys. Chem. C *123*, 5421-5432. 10.1021/acs.jpcc.8b11070.
26. Flaherty, D.W., Hibbitts, D.D., and Iglesia, E. (2014). Metal-catalyzed C-C bond cleavage in alkanes: effects of methyl substitution on transition-state structures and stability. J. Am. Chem. Soc. *136*, 9664-9676. 10.1021/ja5037429.
27. Mason, A.H., Motta, A., Das, A., Ma, Q., Bedzyk, M.J., Kratish, Y., and Marks, T. (2021). Facile Polyolefin Plastics Hydrogenolysis Catalyzed by a Surface Electrophilic d0 Hydride. American Chemical Society (ACS).
28. Ballarini, A.D., de Miguel, S.R., Castro, A.A., and Scelza, O.A. (2013). n-Decane dehydrogenation on Pt, PtSn and PtGe supported on spinels prepared by different methods of synthesis. Appl. Catal., A *467*, 235-245. 10.1016/j.apcata.2013.07.030.
29. Li, H., Wang, L., Dai, Y., Pu, Z., Lao, Z., Chen, Y., Wang, M., Zheng, X., Zhu, J., Zhang, W., et al. (2018). Synergetic interaction between neighbouring platinum monomers in CO2 hydrogenation. Nat Nanotechnol *13*, 411-417. 10.1038/s41565-018-0089-z.
30. Lucci, F.R., Liu, J., Marcinkowski, M.D., Yang, M., Allard, L.F., Flytzani-Stephanopoulos, M., and Sykes, E.C. (2015). Selective hydrogenation of 1,3-butadiene on platinum-copper alloys at the single-atom limit. Nat Commun *6*, 8550. 10.1038/ncomms9550.
31. Sun, G., Zhao, Z.J., Mu, R., Zha, S., Li, L., Chen, S., Zang, K., Luo, J., Li, Z., Purdy, S.C., et al. (2018). Breaking the scaling relationship via thermally stable Pt/Cu single atom alloys for catalytic dehydrogenation. Nat Commun *9*, 4454. 10.1038/s41467-018-06967-8.
32. Sun, P., Siddiqi, G., Chi, M., and Bell, A.T. (2010). Synthesis and characterization of a new catalyst Pt/Mg(Ga)(Al)O for alkane dehydrogenation. J. Catal. *274*, 192-199. 10.1016/j.jcat.2010.06.017.
33. Ertem, S.P., Onuoha, C.E., Wang, H., Hillmyer, M.A., Reineke, T.M., Lodge, T.P., and Bates, F.S. (2020). Hydrogenolysis of Linear Low-Density Polyethylene during Heterogeneous Catalytic Hydrogen–Deuterium Exchange. Macromolecules *53*, 6043-6055. 10.1021/acs.macromol.0c00696.
34. Tennakoon, A., Wu, X., Paterson, A.L., Patnaik, S., Pei, Y., LaPointe, A.M., Ammal, S.C., Hackler, R.A., Heyden, A., Slowing, I.I., et al. (2020). Catalytic upcycling of high-density polyethylene via a processive mechanism. Nat. Catal. *3*, 893-901. 10.1038/s41929-020-00519-4.
35. Wu, X., Tennakoon, A., Yappert, R., Esveld, M., Ferrandon, M.S., Hackler, R.A., LaPointe, A.M., Heyden, A., Delferro, M., Peters, B., et al. (2022). Size-Controlled Nanoparticles Embedded in a Mesoporous Architecture Leading to Efficient and Selective Hydrogenolysis of Polyolefins. J. Am. Chem. Soc. *144*, 5323-5334. 10.1021/jacs.1c11694.
36. Liu, S., Kots, P.A., Vance, B.C., Danielson, A., and Vlachos, D.G. (2021). Plastic waste to fuels by hydrocracking at mild conditions. Sci Adv *7*, 9, eabf8283. 10.1126/sciadv.abf8283.

37. Vance, B.C., Kots, P.A., Wang, C., Hinton, Z.R., Quinn, C.M., Epps, T.H., Korley, L.T.J., and Vlachos, D.G. (2021). Single pot catalyst strategy to branched products via adhesive isomerization and hydrocracking of polyethylene over platinum tungstated zirconia. Appl. Catal., B. *299*, 13, 120483. 10.1016/j.apcatb.2021.120483.
38. Sun, M., Zhu, L., Liu, W., Zhao, X., Zhang, Y., Luo, H., Miao, G., Li, S., Yin, S., and Kong, L. (2022). Efficient upgrading of polyolefin plastics into C5–C12 gasoline alkanes over a Pt/W/Beta catalyst. Sustainable Energy Fuels *6*, 271-275. 10.1039/d1se01778k.
39. Utami, M., Wijaya, K., and Trisunaryanti, W. (2018). Pt-promoted sulfated zirconia as catalyst for hydrocracking of LDPE plastic waste into liquid fuels. Mater. Chem. Phys. *213*, 548-555. 10.1016/j.matchemphys.2018.03.055.
40. Cecchin, G., Morini, G., and Piemontesi, F. (2003). Ziegler-Natta Catalysts. In Kirk-Othmer Encyclopedia of Chemical Technology. 10.1002/0471238961.2609050703050303.a01.
41. Arlman, E. (1964). Ziegler-Natta catalysis II. Surface structure of layer-lattice transition metal chlorides. J. Catal. *3*, 89-98. 10.1016/0021-9517(64)90096-x.
42. Burwell, R.L., and Pearson, R.G. (2002). The Principle of Microscopic Reversibility. J. Phys. Chem. *70*, 300-302. 10.1021/j100873a508.
43. Corker, J., Lefebvre, F., Lécuyer, C., Dufaud, V., Quignard, F., Choplin, A., Evans, J., and Basset, J.-M. (1996). Catalytic Cleavage of the C-H and C-C Bonds of Alkanes by Surface Organometallic Chemistry: An EXAFS and IR Characterization of a Zr-H Catalyst. Science *271*, 966-969. 10.1126/science.271.5251.966.
44. Jia, C., Xie, S., Zhang, W., Intan, N.N., Sampath, J., Pfaendtner, J., and Lin, H. (2021). Deconstruction of high-density polyethylene into liquid hydrocarbon fuels and lubricants by hydrogenolysis over Ru catalyst. Chem Catalysis *1*, 437-455. 10.1016/j.checat.2021.04.002.
45. Sinfelt, J.H. (1973). Specificity in Catalytic Hydrogenolysis by Metals. In Adv. Catal., D.D. Eley, H. Pines, and P.B. Weisz, eds. (Academic Press), pp. 91-119. https://doi.org/10.1016/S0360-0564(08)60299-0.
46. Kots, P.A., Liu, S., Vance, B.C., Wang, C., Sheehan, J.D., and Vlachos, D.G. (2021). Polypropylene Plastic Waste Conversion to Lubricants over Ru/TiO2 Catalysts. ACS Catal. *11*, 8104-8115. 10.1021/acscatal.1c00874.
47. Nakaji, Y., Tamura, M., Miyaoka, S., Kumagai, S., Tanji, M., Nakagawa, Y., Yoshioka, T., and Tomishige, K. (2021). Low-temperature catalytic upgrading of waste polyolefinic plastics into liquid fuels and waxes. Appl. Catal., B. *285*, 9, 119805. 10.1016/j.apcatb.2020.119805.
48. Rorrer, J.E., Troyano-Valls, C., Beckham, G.T., and Román-Leshkov, Y. (2021). Hydrogenolysis of Polypropylene and Mixed Polyolefin Plastic Waste over Ru/C to Produce Liquid Alkanes. ACS Sustain. Chem. Eng. *9*, 11661-11666. 10.1021/acssuschemeng.1c03786.
49. Lapuerta, M., Hernández, J.J., and Sarathy, S.M. (2016). Effects of methyl substitution on the auto-ignition of C16 alkanes. Combust. Flame *164*, 259-269. 10.1016/j.combustflame.2015.11.024.

50. Wang, C., Xie, T., Kots, P.A., Vance, B.C., Yu, K., Kumar, P., Fu, J., Liu, S., Tsilomelekis, G., Stach, E.A., et al. (2021). Polyethylene Hydrogenolysis at Mild Conditions over Ruthenium on Tungstated Zirconia. JACS Au *1*, 1422-1434. 10.1021/jacsau.1c00200.
51. Jing, Y., Wang, Y., Furukawa, S., Xia, J., Sun, C., Hulsey, M.J., Wang, H., Guo, Y., Liu, X., and Yan, N. (2021). Towards the Circular Economy: Converting Aromatic Plastic Waste Back to Arenes over a Ru/Nb2 O5 Catalyst. Angew Chem Int Ed Engl *60*, 5527-5535. 10.1002/anie.202011063.
52. Dong, L., Lin, L., Han, X., Si, X., Liu, X., Guo, Y., Lu, F., Rudić, S., Parker, S.F., Yang, S., and Wang, Y. (2019). Breaking the Limit of Lignin Monomer Production via Cleavage of Interunit Carbon–Carbon Linkages. Chem *5*, 1521-1536. 10.1016/j.chempr.2019.03.007.
53. Barnard, E., Rubio Arias, J.J., and Thielemans, W. (2021). Chemolytic depolymerisation of PET: a review. Green Chem. *23*, 3765-3789. 10.1039/d1gc00887k.
54. Milstein, D. (2010). Discovery of Environmentally Benign Catalytic Reactions of Alcohols Catalyzed by Pyridine-Based Pincer Ru Complexes, Based on Metal–Ligand Cooperation. Top. Catal. *53*, 915-923. 10.1007/s11244-010-9523-7.
55. Balaraman, E., Fogler, E., and Milstein, D. (2012). Efficient hydrogenation of biomass-derived cyclic di-esters to 1,2-diols. Chem Commun (Camb) *48*, 1111-1113. 10.1039/c1cc15778g.
56. Krall, E.M., Klein, T.W., Andersen, R.J., Nett, A.J., Glasgow, R.W., Reader, D.S., Dauphinais, B.C., Mc Ilrath, S.P., Fischer, A.A., Carney, M.J., et al. (2014). Controlled hydrogenative depolymerization of polyesters and polycarbonates catalyzed by ruthenium(II) PNN pincer complexes. Chem Commun (Camb) *50*, 4884-4887. 10.1039/c4cc00541d.
57. Papageorgiou, D.G., Roumeli, E., Chrissafis, K., Lioutas, C., Triantafyllidis, K., Bikiaris, D., and Boccaccini, A.R. (2014). Thermal degradation kinetics and decomposition mechanism of PBSu nanocomposites with silica-nanotubes and strontium hydroxyapatite nanorods. Phys. Chem. Chem. Phys. *16*, 4830-4842. 10.1039/c3cp55103b.
58. Zhang, H., Kang, S., Fu, J., He, Y., Huang, X., Chang, J., and Xu, Y. (2021). Valorization of poly(butylene succinate) to tetrahydrofuran via one-pot catalytic hydrogenolysis. React. Chem. Eng. *6*, 465-470. 10.1039/d0re00441c.
59. Oya, S., Kanno, D., Watanabe, H., Tamura, M., Nakagawa, Y., and Tomishige, K. (2015). Catalytic production of branched small alkanes from biohydrocarbons. ChemSusChem *8*, 2472-2475. 10.1002/cssc.201500375.
60. Nakaji, Y., Nakagawa, Y., Tamura, M., and Tomishige, K. (2018). Regioselective hydrogenolysis of alga-derived squalane over silica-supported ruthenium-vanadium catalyst. Fuel Process. Technol. *176*, 249-257. 10.1016/j.fuproc.2018.03.038.
61. Wang, S., Ma, S., Qiu, J., Tian, A., Li, Q., Xu, X., Wang, B., Lu, N., Liu, Y., and Zhu, J. (2021). Upcycling of post-consumer polyolefin plastics to covalent adaptable

networks via in situ continuous extrusion cross-linking. Green Chem. *23*, 2931-2937. 10.1039/d0gc04337k.
62. Sinfelt, J.H. (1991). Catalytic hydrogenolysis on metals. Catal. Lett. *9*, 159-171. 10.1007/bf00773174.
63. Shetty, M., Zanchet, D., Green, W.H., and Roman-Leshkov, Y. (2019). Cooperative Co(0) /Co(II) Sites Stabilized by a Perovskite Matrix Enable Selective C-O and C-C bond Hydrogenolysis of Oxygenated Arenes. ChemSusChem *12*, 2171-2175. 10.1002/cssc.201900664.
64. Rohrer, J.C., and Sinfelt, J.H. (1962). Catalytic Hydrogenolysis of Benzene and Toluene. J. Phys. Chem. *66*, 1190-1192. 10.1021/j100812a505.
65. Sinfelt, J.H. (1964). Hydrogenolysis of Ethane over Supported Platinum. J. Phys. Chem. *68*, 344-&. DOI 10.1021/j100784a023.
66. Sinfelt, J.H. (1969). Catalytic Hydrogenolysis over Supported Metals. Catal. Rev. *3*, 175-&.
67. Sinfelt, J.H., Yates, D.J.C., and Carter, J.L. (1972). Catalytic Hydrogenolysis and Dehydrogenation over Copper-Nickel Alloys. J. Catal. *24*, 283-&. Doi 10.1016/0021-9517(72)90072-3.
68. Hibbitts, D.D., Flaherty, D.W., and Iglesia, E. (2016). Effects of Chain Length on the Mechanism and Rates of Metal-Catalyzed Hydrogenolysis of n-Alkanes. J. Phys. Chem. C *120*, 8125-8138. 10.1021/acs.jpcc.6b00323.
69. Flaherty, D.W., Hibbitts, D.D., Gurbuz, E.I., and Iglesia, E. (2014). Theoretical and kinetic assessment of the mechanism of ethane hydrogenolysis on metal surfaces saturated with chemisorbed hydrogen. J. Catal. *311*, 350-356. 10.1016/j.jcat.2013.11.026.
70. Flaherty, D.W., Uzun, A., and Iglesia, E. (2015). Catalytic Ring Opening of Cycloalkanes on Ir Clusters: Alkyl Substitution Effects on the Structure and Stability of C-C Bond Cleavage Transition States. J. Phys. Chem. C *119*, 2597-2613. 10.1021/jp511688x.
71. Hibbitts, D.D., Flaherty, D.W., and Iglesia, E. (2016). Role of Branching on the Rate and Mechanism of C-C Cleavage in Alkanes on Metal Surfaces. ACS Catal. *6*, 469-482. 10.1021/acscatal.5b01950.
72. Sinfelt, J. (1967). Catalytic hydrogenolysis of ethane over the noble metals of Group VIII. J. Catal. *8*, 82-90. 10.1016/0021-9517(67)90284-9.
73. Sinfelt, J.H., Taylor, W.F., and Yates, D.J.C. (2002). Catalysis over Supported Metals. III. Comparison of Metals of Known Surface Area for Ethane Hydrogenolysis. J. Phys. Chem. *69*, 95-101. 10.1021/j100885a016.
74. Morikawa, K., Benedict, W.S., and Taylor, H.S. (2002). The Activation of Specific Bonds in Complex Molecules at Catalytic Surfaces. II. The Carbon-Hydrogen and Carbon-Carbon Bonds in Ethane and Ethane-d. J. Am. Chem. Soc. *58*, 1795-1800. 10.1021/ja01300a084.
75. Kemball, C., and Taylor, H.S. (1948). The catalytic decomposition of ethane and ethane–hydrogen mixtures. J. Am. Chem. Soc. *70*, 345-351.
76. Sinfelt, J. (1972). Kinetics of ethane hydrogenolysis. J. Catal. *27*, 468-471.

77. Flaherty, D.W., and Iglesia, E. (2013). Transition-state enthalpy and entropy effects on reactivity and selectivity in hydrogenolysis of n-alkanes. J. Am. Chem. Soc. *135*, 18586-18599. 10.1021/ja4093743.
78. Ooka, H., Huang, J., and Exner, K.S. (2021). The Sabatier Principle in Electrocatalysis: Basics, Limitations, and Extensions. Front. Energy Res. *9*. 10.3389/fenrg.2021.654460.
79. Nakagawa, Y., Oya, S.I., Kanno, D., Nakaji, Y., Tamura, M., and Tomishige, K. (2017). Regioselectivity and Reaction Mechanism of Ru-Catalyzed Hydrogenolysis of Squalane and Model Alkanes. ChemSusChem *10*, 189-198. 10.1002/cssc.201601204.
80. Oenema, J., Harmel, J., Velez, R.P., Meijerink, M.J., Eijsvogel, W., Poursaeidesfahani, A., Vlugt, T.J.H., Zecevic, J., and de Jong, K.P. (2020). Influence of Nanoscale Intimacy and Zeolite Micropore Size on the Performance of Bifunctional Catalysts for n-Heptane Hydroisomerization. ACS Catal *10*, 14245-14257. 10.1021/acscatal.0c03138.
81. Al-Salem, S.M., Antelava, A., Constantinou, A., Manos, G., and Dutta, A. (2017). A review on thermal and catalytic pyrolysis of plastic solid waste (PSW). J Environ Manage *197*, 177-198. 10.1016/j.jenvman.2017.03.084.
82. Maqsood, T., Dai, J., Zhang, Y., Guang, M., and Li, B. (2021). Pyrolysis of plastic species: A review of resources and products. J. Anal. Appl. Pyrolysis *159*, 12, 105295. 10.1016/j.jaap.2021.105295.
83. Damayanti, and Wu, H.S. (2021). Strategic Possibility Routes of Recycled PET. Polymers (Basel) *13*, 37, 1475. 10.3390/polym13091475.
84. Butler, E., Devlin, G., and McDonnell, K. (2011). Waste Polyolefins to Liquid Fuels via Pyrolysis: Review of Commercial State-of-the-Art and Recent Laboratory Research. Waste Biomass Valorization *2*, 227-255. 10.1007/s12649-011-9067-5.
85. Eschenbacher, A., Varghese, R.J., Delikonstantis, E., Mynko, O., Goodarzi, F., Enemark-Rasmussen, K., Oenema, J., Abbas-Abadi, M.S., Stefanidis, G.D., and Van Geem, K.M. (2022). Highly selective conversion of mixed polyolefins to valuable base chemicals using phosphorus-modified and steam-treated mesoporous HZSM-5 zeolite with minimal carbon footprint. Appl. Catal., B. *309*, 15, 121251. 10.1016/j.apcatb.2022.121251.
86. Garcia-Nunez, J.A., Pelaez-Samaniego, M.R., Garcia-Perez, M.E., Fonts, I., Abrego, J., Westerhof, R.J.M., and Garcia-Perez, M. (2017). Historical Developments of Pyrolysis Reactors: A Review. Energy Fuels *31*, 5751-5775. 10.1021/acs.energyfuels.7b00641.
87. Miandad, R., Barakat, M.A., Aburiazaiza, A.S., Rehan, M., and Nizami, A.S. (2016). Catalytic pyrolysis of plastic waste: A review. Process Saf. Environ. Prot. *102*, 822-838. 10.1016/j.psep.2016.06.022.
88. Audisio, G., Bertini, F., Beltrame, P.L., and Carniti, P. (1990). Catalytic degradation of polymers: Part III—Degradation of polystyrene. Polym. Degrad. Stab. *29*, 191-200. 10.1016/0141-3910(90)90030-b.
89. Sakata, Y., Azhar Uddin, M., Muto, A., Kanada, Y., Koizumi, K., and Murata, K. (1997). Catalytic degradation of polyethylene into fuel oil over mesoporous silica

(KFS-16) catalyst. J. Anal. Appl. Pyrolysis *43*, 15-25. 10.1016/s0165-2370(97)00052-1.

90. Azhar Uddin, M., Sakata, Y., Muto, A., Shiraga, Y., Koizumi, K., Kanada, Y., and Murata, K. (1998). Catalytic degradation of polyethylene and polypropylene into liquid hydrocarbons with mesoporous silica. Microporous Mesoporous Mater. *21*, 557-564. 10.1016/s1387-1811(98)00036-5.
91. Zhang, Z., Gora-Marek, K., Watson, J.S., Tian, J., Ryder, M.R., Tarach, K.A., López-Pérez, L., Martínez-Triguero, J., and Melián-Cabrera, I. (2019). Recovering waste plastics using shape-selective nano-scale reactors as catalysts. Nat. Sustain. *2*, 39-42. 10.1038/s41893-018-0195-9.
92. Serrano, D. (2004). Feedstock recycling of agriculture plastic film wastes by catalytic cracking. Appl. Catal., B. *49*, 257-265. 10.1016/j.apcatb.2003.12.014.
93. Li, H.A.-V., H. A.; Allen , R. D.; Bai, X.; Benson, C. H.; Beckham, G. T.; Bradshaw, S. L.; Brown, J. L.; Brown, R. C.; Sanchez Castillo, M. A.; Cecon, V. S.; Curley, J. B.; Curtzwiler, G. W.; Dong, S.; Gaddameedi, S.; Garcia, J. E.; Hermans, I.; Kim, M. S.; Ma, J.; Mark, L. O.; Mavrikakis, M.; Olafasakin, O. O.; Osswald, T. A.; Papanikolaou, K. G.; Radhakrishnan, H.; Sánchez-Rivera, K. L.; Tumu, K. N.; Van Lehn, R. C.; Vorst, K. L.; Wright, M. M.; Wu, J.; Zavala, V. M.; Zhou, P.; Huber, G. W. (2022). Expanding Plastics Recycling Technologies: Chemical Aspects, Technology Status and Challenges. ChemRxiv.
94. Singh, M.V. (2018). Waste and virgin high-density poly(ethylene) into renewable hydrocarbons fuel by pyrolysis-catalytic cracking with a CoCO3 catalyst. J. Anal. Appl. Pyrolysis *134*, 150-161. 10.1016/j.jaap.2018.06.003.
95. Singh, M.V., Kumar, S., and Sarker, M. (2018). Waste HD-PE plastic, deformation into liquid hydrocarbon fuel using pyrolysis-catalytic cracking with a CuCO3 catalyst. Sustainable Energy Fuels *2*, 1057-1068. 10.1039/c8se00040a.
96. Sun, K., Huang, Q., Meng, X., Chi, Y., and Yan, J. (2018). Catalytic Pyrolysis of Waste Polyethylene into Aromatics by H3PO4-Activated Carbon. Energy Fuels *32*, 9772-9781. 10.1021/acs.energyfuels.8b02091.
97. Wojciechowski, B.W. (1998). The Reaction Mechanism of Catalytic Cracking: Quantifying Activity, Selectivity, and Catalyst Decay. Catal. Rev. *40*, 209-328. 10.1080/01614949808007110.
98. Zavala-Gutiérrez, J., Pérez-Camacho, O., Villarreal-Cárdenas, L., and Saldívar-Guerra, E. (2019). Mathematical Modeling of the Catalytic Pyrolysis of High-Density Polyethylene in a Plug-Flow Tubular Reactor. Ind. Eng. Chem. Res. *58*, 19050-19060. 10.1021/acs.iecr.9b04025.
99. White, R.L. (2006). Acid-Catalyzed Cracking of Polyolefins: Primary Reaction Mechanisms. In Feedstock Recycling and Pyrolysis of Waste Plastics, pp. 43-72. 10.1002/0470021543.ch2.
100. Spychaj, T. (2002). Chemical Recycling of PET: Methods and Products. In Handbook of Thermoplastic Polyesters, pp. 1252-1290. 10.1002/3527601961.ch27.

101. Al-Sabagh, A.M., Yehia, F.Z., Eshaq, G., Rabie, A.M., and ElMetwally, A.E. (2016). Greener routes for recycling of polyethylene terephthalate. Egypt. J. Pet. *25*, 53-64. https://doi.org/10.1016/j.ejpe.2015.03.001.
102. Ügdüler, S., Van Geem, K.M., Denolf, R., Roosen, M., Mys, N., Ragaert, K., and De Meester, S. (2020). Towards closed-loop recycling of multilayer and coloured PET plastic waste by alkaline hydrolysis. Green Chem. *22*, 5376-5394. 10.1039/d0gc00894j.
103. Ghorbantabar, S., Ghiass, M., Yaghobi, N., and Bouhendi, H. (2021). Investigation of conventional analytical methods for determining conversion of polyethylene terephthalate waste degradation via aminolysis process. J. Mater. Cycles Waste Manage. *23*, 526-536. 10.1007/s10163-020-01149-5.
104. Bäckström, E., Odelius, K., and Hakkarainen, M. (2021). Ultrafast microwave assisted recycling of PET to a family of functional precursors and materials. Eur. Polym. J. *151*, 110441. 10.1016/j.eurpolymj.2021.110441.
105. Liu, M., Guo, J., Gu, Y., Gao, J., Liu, F., and Yu, S. (2018). Pushing the Limits in Alcoholysis of Waste Polycarbonate with DBU-Based Ionic Liquids under Metal- and Solvent-Free Conditions. ACS Sustain. Chem. Eng. *6*, 13114-13121. 10.1021/acssuschemeng.8b02650.
106. Saito, K., Jehanno, C., Meabe, L., Olmedo-Martínez, J.L., Mecerreyes, D., Fukushima, K., and Sardon, H. (2020). From plastic waste to polymer electrolytes for batteries through chemical upcycling of polycarbonate. J. Mater. Chem. A *8*, 13921-13926. 10.1039/d0ta03374j.
107. Jehanno, C., Demarteau, J., Mantione, D., Arno, M.C., Ruiperez, F., Hedrick, J.L., Dove, A.P., and Sardon, H. (2020). Synthesis of Functionalized Cyclic Carbonates through Commodity Polymer Upcycling. ACS Macro Lett *9*, 443-447. 10.1021/acsmacrolett.0c00164.
108. Demarteau, J., Olazabal, I., Jehanno, C., and Sardon, H. (2020). Aminolytic upcycling of poly(ethylene terephthalate) wastes using a thermally-stable organocatalyst. Polym. Chem. *11*, 4875-4882. 10.1039/d0py00067a.
109. Payne, J., and Jones, M.D. (2021). The Chemical Recycling of Polyesters for a Circular Plastics Economy: Challenges and Emerging Opportunities. ChemSusChem *14*, 4041-4070. 10.1002/cssc.202100400.
110. Kale, G., Auras, R., Singh, S.P., and Narayan, R. (2007). Biodegradability of polylactide bottles in real and simulated composting conditions. Polym. Test. *26*, 1049-1061. 10.1016/j.polymertesting.2007.07.006.
111. Niaounakis, M. (2019). Recycling of biopolymers – The patent perspective. Eur. Polym. J. *114*, 464-475. 10.1016/j.eurpolymj.2019.02.027.
112. Piemonte, V., and Gironi, F. (2012). Kinetics of Hydrolytic Degradation of PLA. J. Polym. Environ. *21*, 313-318. 10.1007/s10924-012-0547-x.
113. Hirao, K., Shimamoto, Y., Nakatsuchi, Y., and Ohara, H. (2010). Hydrolysis of poly(l-lactic acid) using microwave irradiation. Polym. Degrad. Stab. *95*, 86-88. 10.1016/j.polymdegradstab.2009.10.003.
114. Tang, H., Li, N., Li, G., Wang, A., Cong, Y., Xu, G., Wang, X., and Zhang, T. (2019). Synthesis of gasoline and jet fuel range cycloalkanes and aromatics from

poly(ethylene terephthalate) waste. Green Chem. *21*, 2709-2719. 10.1039/c9gc00571d.
115. Lu, S., Jing, Y., Feng, B., Guo, Y., Liu, X., and Wang, Y. (2021). H2 -free Plastic Conversion: Converting PET back to BTX by Unlocking Hidden Hydrogen. ChemSusChem *14*, 4242-4250. 10.1002/cssc.202100196.
116. Li, Y., Wang, M., Liu, X., Hu, C., Xiao, D., and Ma, D. (2022). Catalytic Transformation of PET and CO2 into High-Value Chemicals. Angew Chem Int Ed Engl *61*, e202117205. 10.1002/anie.202117205.
117. Tang, H., Hu, Y., Li, G., Wang, A., Xu, G., Yu, C., Wang, X., Zhang, T., and Li, N. (2019). Synthesis of jet fuel range high-density polycycloalkanes with polycarbonate waste. Green Chem. *21*, 3789-3795. 10.1039/c9gc01627a.
118. Wang, L., Li, G., Cong, Y., Wang, A., Wang, X., Zhang, T., and Li, N. (2021). Direct synthesis of a jet fuel range dicycloalkane by the aqueous phase hydrodeoxygenation of polycarbonate. Green Chem. *23*, 3693-3699. 10.1039/d1gc00353d.
119. Walker, T.W., Frelka, N., Shen, Z., Chew, A.K., Banick, J., Grey, S., Kim, M.S., Dumesic, J.A., Van Lehn, R.C., and Huber, G.W. (2020). Recycling of multilayer plastic packaging materials by solvent-targeted recovery and precipitation. Sci Adv *6*, eaba7599. 10.1126/sciadv.aba7599.
120. Rorrer, N.A., Nicholson, S., Carpenter, A., Biddy, M.J., Grundl, N.J., and Beckham, G.T. (2019). Combining Reclaimed PET with Bio-based Monomers Enables Plastics Upcycling. Joule *3*, 1006-1027. 10.1016/j.joule.2019.01.018.
121. Vidal, V.V., Theolier, A., Thivolle-Cazat, J., and Basset, J.M. (1997). Metathesis of Alkanes Catalyzed by Silica-Supported Transition Metal Hydrides. Science *276*, 99-102. 10.1126/science.276.5309.99.
122. Burnett, R. (1973). Mechanism and poisoning of the molecular redistribution reaction of alkanes with a dual-functional catalyst system. J. Catal. *31*, 55-64. 10.1016/0021-9517(73)90270-4.
123. Jia, X.Q., Qin, C., Friedberger, T., Guan, Z.B., and Huang, Z. (2016). Efficient and selective degradation of polyethylenes into liquid fuels and waxes under mild conditions. Sci. Adv. *2*, 7, e1501591. 10.1126/sciadv.1501591.
124. Ellis, L.D., Orski, S.V., Kenlaw, G.A., Norman, A.G., Beers, K.L., Román-Leshkov, Y., and Beckham, G.T. (2021). Tandem Heterogeneous Catalysis for Polyethylene Depolymerization via an Olefin-Intermediate Process. ACS Sustain. Chem. Eng. *9*, 623-628. 10.1021/acssuschemeng.0c07612.
125. Kar, G.P., Saed, M.O., and Terentjev, E.M. (2020). Scalable upcycling of thermoplastic polyolefins into vitrimers through transesterification. J. Mater. Chem. A *8*, 24137-24147. 10.1039/d0ta07339c.
126. Brutman, J.P., Delgado, P.A., and Hillmyer, M.A. (2014). Polylactide Vitrimers. ACS Macro Lett *3*, 607-610. 10.1021/mz500269w.
127. Capelot, M., Unterlass, M.M., Tournilhac, F., and Leibler, L. (2012). Catalytic Control of the Vitrimer Glass Transition. ACS Macro Lett *1*, 789-792. 10.1021/mz300239f.

128. Chen, L., Malollari, K.G., Uliana, A., Sanchez, D., Messersmith, P.B., and Hartwig, J.F. (2021). Selective, Catalytic Oxidations of C–H Bonds in Polyethylenes Produce Functional Materials with Enhanced Adhesion. Chem *7*, 137-145. 10.1016/j.chempr.2020.11.020.
129. Williamson, J.B., Lewis, S.E., Johnson III, R.R., Manning, I.M., and Leibfarth, F.A. (2019). C−H Functionalization of Commodity Polymers. Angew. Chem. Int. Ed. *58*, 8654-8668. https://doi.org/10.1002/anie.201810970.
130. Pichler, C.M., Bhattacharjee, S., Rahaman, M., Uekert, T., and Reisner, E. (2021). Conversion of Polyethylene Waste into Gaseous Hydrocarbons via Integrated Tandem Chemical-Photo/Electrocatalytic Processes. ACS Catal *11*, 9159-9167. 10.1021/acscatal.1c02133.
131. Chen, F., Shetty, M., Wang, M., Shi, H., Liu, Y.S., Camaioni, D.M., Gutierrez, O.Y., and Lercher, J.A. (2021). Differences in Mechanism and Rate of Zeolite-Catalyzed Cyclohexanol Dehydration in Apolar and Aqueous Phase. ACS Catal. *11*, 2879-2888. 10.1021/acscatal.0c05674.
132. Shetty, M., Wang, H.M., Chen, F., Jaegers, N., Liu, Y., Camaioni, D.M., Gutierrez, O.Y., and Lercher, J.A. (2021). Directing the Rate-Enhancement for Hydronium Ion Catalyzed Dehydration via Organization of Alkanols in Nanoscopic Confinements. Angew. Chem. Int. Ed. *60*, 2304-2311. 10.1002/anie.202009835.
133. Wang, H., Tian, P., Chen, Z., Wu, S., Yang, W., Yu, Q., and Zhou, J. (2018). Effect of coke formation on catalytic activity tests for catalytic combustion of toluene: the difficulty of measuring TOF and T98 accurately. Chem. Eng. Commun. *206*, 22-32. 10.1080/00986445.2018.1470510.
134. Date, A.W. (2020). Analytic Combustion: With Thermodynamics, Chemical Kinetics and Mass Transfer, 2nd Edition (Springer).

# *List of Tables*

# *List of Figures and Captions*

# *Graphical Abstract*